Cell

Transplantation of chemically induced pluripotent stem-cell-derived islets under abdominal anterior rectus sheath in a type 1 diabetes patient

Graphical abstract

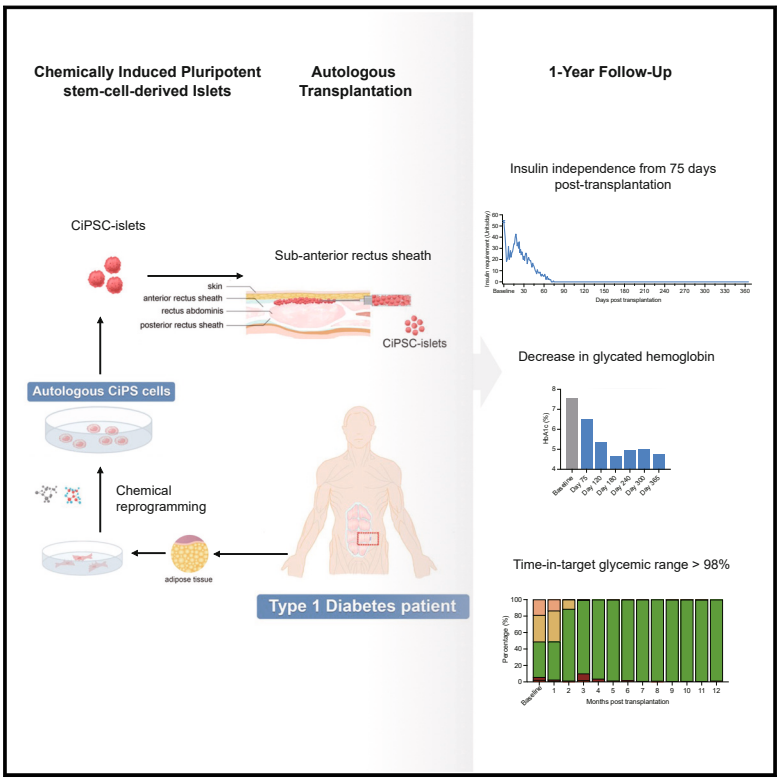

Highlights

- Patient-derived islets were generated with chemically induced pluripotent stem cells
- Transplantation of these islets to an abdominal site led to engraftment in one patient
- Exogenous insulin-independent glycemic control was restored in the patient
- All safety and efficacy clinical endpoints were met at 1-year follow-up of the patient

Authors

Shusen Wang, Yuanyuan Du, Boya Zhang, ..., Shuang Wang, Hongkui Deng, Zhongyang Shen

Correspondence

shusen@vip.163.com (S.W.), hongkui_deng@pku.edu.cn (H.D.), zhongyangshen@vip.sina.com (Z.S.)

In brief

Chemically induced stem-cell-derived islets were transplanted beneath the abdominal anterior rectus sheath in one patient with type 1 diabetes, resulting in tolerable safety and promising restoration of exogenous-insulin-independent glycemic control at 1-year follow-up.

Wang et al., 2024, Cell *187*, 6152–6164
October 31, 2024
https://doi.org/10.1016/j.cell.2024.09.004

CellPress

CellPress

Cell

Article

Transplantation of chemically induced pluripotent stem-cell-derived islets under abdominal anterior rectus sheath in a type 1 diabetes patient

Shusen Wang,[1,10,*] Yuanyuan Du,[2,3,10] Boya Zhang,[1,10] Gaofan Meng,[2,3,10] Zewen Liu,[1,10] Soon Yi Liew,[2,3,10] Rui Liang,[1,10] Zhengyuan Zhang,[2,10] Xiangheng Cai,[1,10] Shuangshuang Wu,[3,10] Wei Gao,[1,10] Dewei Zhuang,[3] Jiaqi Zou,[1] Hui Huang,[3] Mingyang Wang,[5] Xiaofeng Wang,[3] Xuelian Wang,[1] Ting Liang,[3] Tengli Liu,[1] Jiabin Gu,[3] Na Liu,[1] Yanling Wei,[3] Xuejie Ding,[1] Yue Pu,[3] Yixiang Zhan,[1] Yu Luo,[3] Peng Sun,[1] Shuangshuang Xie,[6] Jiuxia Yang,[1] Yiqi Weng,[7] Chunlei Zhou,[8] Zhenglu Wang,[1] Shuang Wang,[9] Hongkui Deng,[2,4,11,*] and Zhongyang Shen[1,*]

[1]Research Institute of Transplant Medicine, Organ Transplant Center, Tianjin First Central Hospital, School of Medicine, Nankai University, NHC Key Laboratory for Critical Care Medicine, Key Laboratory of Transplant Medicine, Chinese Academy of Medical Sciences, Tianjin 300192, China

[2]School of Basic Medical Sciences, MOE Engineering Research Center of Regenerative Medicine, State Key Laboratory of Natural and Biomimetic Drugs, Peking University Health Science Center and the MOE Key Laboratory of Cell Proliferation and Differentiation, College of Life Sciences, Peking-Tsinghua Center for Life Sciences, Peking University, Beijing 100191, China

[3]Hangzhou Reprogenix Bioscience, Hangzhou, China

[4]China Changping Laboratory, Beijing 102206, China

[5]Department of Ultrasound, Tianjin First Central Hospital, Nankai University, Tianjin 300192, China

[6]Radiology Department, Tianjin First Central Hospital, Nankai University, Tianjin 300192, China

[7]Department of Anesthesiology, Tianjin First Central Hospital, Nankai University, Tianjin 300192, China

[8]Department of Medical Laboratory, Tianjin First Central Hospital, Nankai University, Tianjin 300192, China

[9]Department of Plastic and Burn, Tianjin First Central Hospital, Nankai University, Tianjin 300192, China

[10]These authors contributed equally

[11]Lead contact

*Correspondence: shusen@vip.163.com (S.W.), hongkui_deng@pku.edu.cn (H.D.), zhongyangshen@vip.sina.com (Z.S.)

https://doi.org/10.1016/j.cell.2024.09.004

SUMMARY

We report the 1-year results from one patient as the preliminary analysis of a first-in-human phase I clinical trial (ChiCTR2300072200) assessing the feasibility of autologous transplantation of chemically induced pluripotent stem-cell-derived islets (CiPSC islets) beneath the abdominal anterior rectus sheath for type 1 diabetes treatment. The patient achieved sustained insulin independence starting 75 days post-transplantation. The patient's time-in-target glycemic range increased from a baseline value of 43.18% to 96.21% by month 4 post-transplantation, accompanied by a decrease in glycated hemoglobin, an indicator of long-term systemic glucose levels at a non-diabetic level. Thereafter, the patient presented a state of stable glycemic control, with time-in-target glycemic range at >98% and glycated hemoglobin at around 5%. At 1 year, the clinical data met all study endpoints with no indication of transplant-related abnormalities. Promising results from this patient suggest that further clinical studies assessing CiPSC-islet transplantation in type 1 diabetes are warranted.

INTRODUCTION

Pluripotent stem cells (PSCs) show remarkable potential as an unlimited cell source for cellular replacement therapies such as islet transplantation, owing to their ability to self-renew and differentiate into functional cell types.[1] The derivation of human induced PSCs (iPSCs) from somatic cells in 2007 marked a groundbreaking advance in the ethical generation of pluripotent stem cells, making patient-derived autologous regenerative medicine possible.[2,3] Recently, we successfully reprogrammed human somatic cells to chemically induced PSCs (CiPSCs).[4,5] Different from conventional iPSCs, which are generated from somatic cells by genetic overexpression of transcription factors, the generation of CiPSCs from somatic cells employs abiotic, small-molecule chemicals as reprogramming factors that are easily manufactured and standardized, non-genome integrating, scalable, and fine-tunable.[6] This approach provides a fundamentally different route to generate human PSCs (hPSCs) that are suitable for therapeutic applications.

In addition to the generation of hPSCs, the development of strategies to induce differentiation of PSCs into functional islet-like cells (hPSC-islets) has been a decades-long pursuit by our

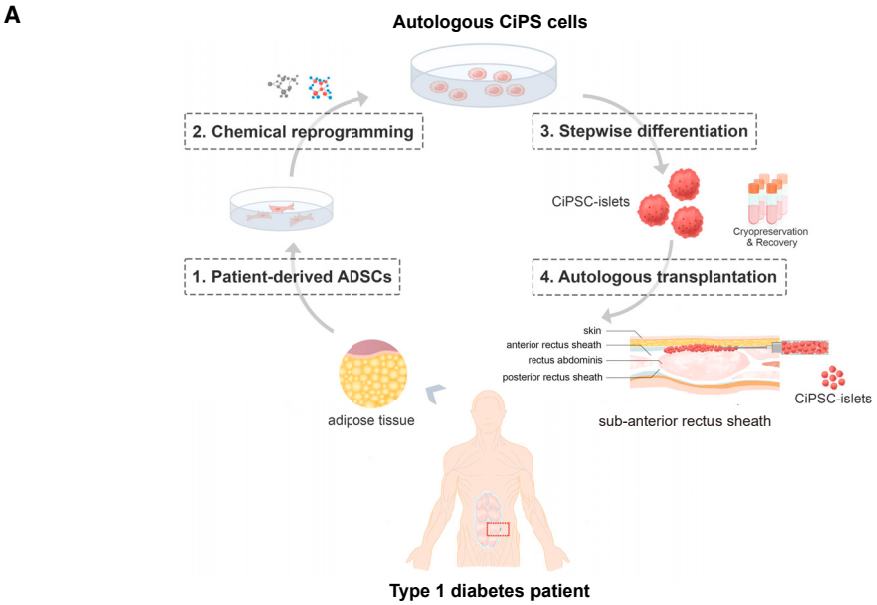

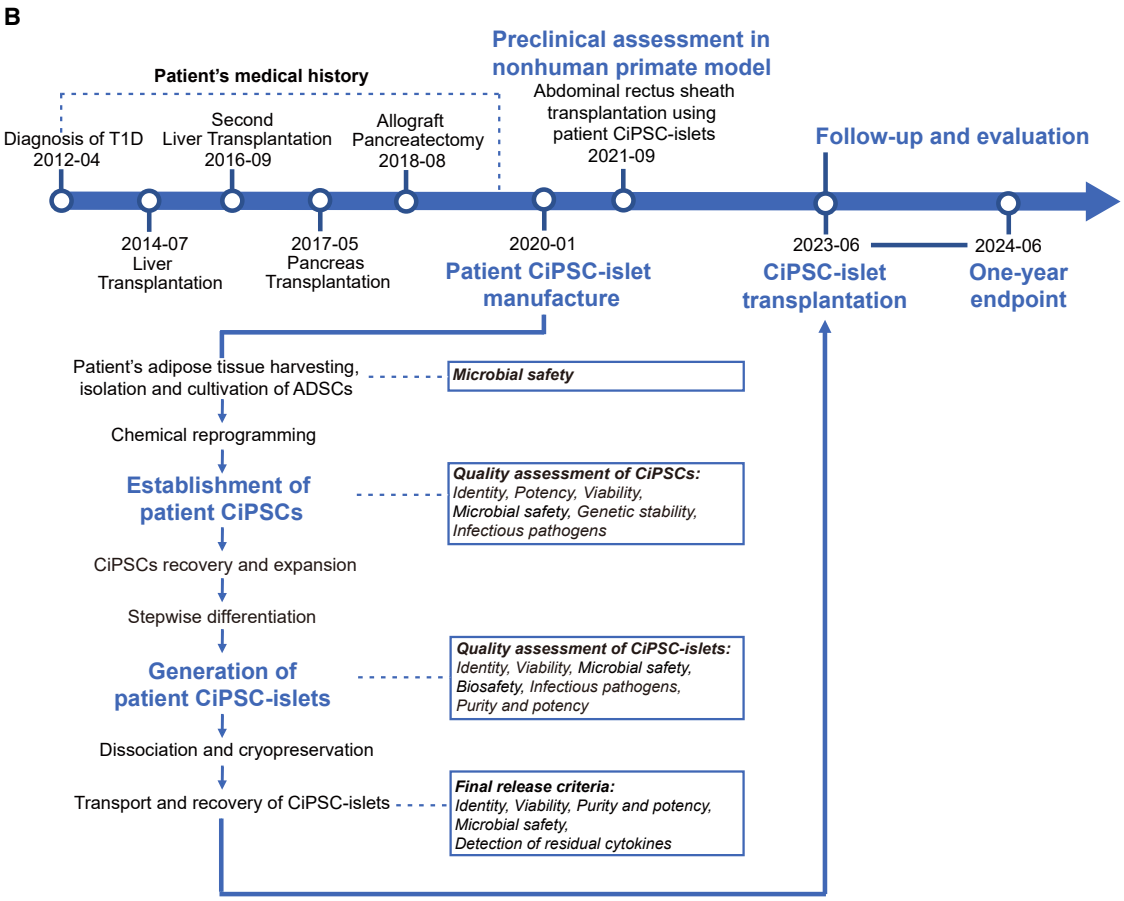

(legend on next page)

group and others. The earliest differentiation protocols focused on deriving insulin-producing β-like cells *in vitro* from embryonic stem cells (ESCs)[7–10] and iPSCs.[11,12] Subsequently, later research focused on efficiently obtaining β-like cells with improved insulin secretion, resulting in the generation of functional hPSC-derived β cells.[13–18] Based on our work using pancreatic development gene-labeled reporter lines,[19] we established a highly efficient, optimized differentiation protocol for the generation of islet-like cells from CiPSCs (CiPSC-islets), whose transcriptomic identity, composition, and insulin secretory function were comparable to that of native human islets.[20] The safety and efficacy of CiPSC-islets were evaluated in two systematic preclinical studies in nonhuman primates, in which amelioration of diabetes and no tumorigenicity during long-term observation were demonstrated, indicating marked therapeutic potential for diabetes treatment.[20,21]

Importantly, in these preclinical studies, we also developed a suitable transplantation strategy for hPSC-islets.[21] Because conventional islet transplantation by infusion into the hepatic portal vein suffers from certain limitations, such as acute graft loss triggered by an instant blood-mediated inflammatory response (IBMIR),[22–24] alternative transplantation sites for more optimum graft survival have been the object of investigation for several years.[25–28] We found that transplantation to an extrahepatic site, underneath the abdominal anterior rectus sheath, led to superior CiPSC-islet survival and maturation, resulting in secretion levels of C-peptide (a marker of endogenous insulin secretion) and stimulation indices approaching those of non-diabetic humans.[21] Other important advantages of this self-contained extraperitoneal transplant site include minimal invasiveness of injection at the site and ease of imaging. Taken together, these studies established a foundation for the clinical translation of CiPSC-islets in human patients.

Here, we report for the first time autologous transplantation of CiPSC-derived islets into a patient with type 1 diabetes (T1D) with immunosuppression as part of an exploratory clinical study, which resulted in sustained insulin independence and restored glycemic control.

RESULTS

Overview of study design

This report presents findings from the first patient enrolled in the ongoing TJFCH-iPS-001 trial (ChiCTR2300072200), which aims to evaluate the safety, tolerability, and efficacy of autologous CiPSC-islets as a treatment strategy for T1D. Briefly, patient-specific CiPSCs were generated by our previously reported chemical reprogramming approach[4] and subsequently differentiated *in vitro* into insulin-producing islet-like cells using our previously established protocol,[20] with in-process quality control (QC) assessments throughout the manufacturing process. Final release criteria-qualified patient CiPSC-islets were transplanted by ultrasound-guided injection into the abdominal anterior rectus sheath of the patient (Figures 1A and 1B).

The primary endpoints of the study included a decrease of glycated hemoglobin (HbA1c) to below 7.0% or a decrease in HbA1c by ≥1% compared with baseline from 90–365 days post-transplantation and no occurrence of severe hypoglycemic events in the subject as well as safety and tolerability assessments. The secondary endpoints included insulin independence and a stimulated C-peptide level of ≥0.3 ng/mL (99.3 pmol/L). This study was approved by the National Health Commission of the People's Republic of China and the Medical Ethics Committee at Tianjin First Central Hospital. All the authors vouch for the completeness and accuracy of the data reported and for the adherence of the study to the protocol.

Study participant

A 25-year-old woman was diagnosed with T1D for 11 years (as of time of transplantation in 2023). Her weight was 75 kg, and her body mass index was 27.3 kg/m^2. Her medical history included two liver transplantations due to cryptogenic cirrhosis in 2014 and 2016, respectively, and a whole pancreas transplantation in 2017 due to unstable glycemic control. The pancreas graft was removed after a year due to severe thrombotic complications (Figure 1B). The patient was under regular immunosuppression for liver transplant maintenance.

Prior to enrollment, the patient's plasma C-peptide levels were below the limit of detection (6.6 pmol/L) under both fasting and glucose-challenged conditions. Despite receiving intensive insulin treatment at a daily dose of 54 ± 0.9 units (mean ± SD) under the supervision of an endocrinologist, the patient was still not able to achieve target glycemic control. Her HbA1c level during the 2 years before enrollment was 7.40%–8.00%, higher than the American Diabetes Association (ADA)'s recommended target for T1D management (<7.0%).[29] Continuous glucose monitoring (CGM) measurements during the three months before transplantation showed severe glucose variability and endangerment by hypoglycemia, and the patient experienced 3 incidences of severe hypoglycemic events in the prior year. Her fasting glucose fluctuated greatly, with an average value of 210 ± 59 mg/dL (mean ± SD). Her time in the target glucose range (TIR) was 43.18% (the ADA target is >70%[29]) during the 3 months prior to the transplantation, and her time in the very low range of blood glucose (<54 mg/dL) was 2.01% (the ADA target is <1%[29]). These data indicated that intensive insulin therapy was insufficient for achieving adequate glycemic control. The patient's clinical presentation, including glycemic lability, β cell depletion, and hypoglycemia, aligned with the indications for clinical islet transplantation.[30]

Figure 1. Transplantation of chemically induced autologous pluripotent stem-cell-derived islets for type 1 diabetes

(A) A schematic diagram depicting the clinical study. Patient-derived iPSCs were generated from adipose-derived mesenchymal stromal cells (ADSCs) isolated from the patient's adipose tissue using a chemical reprogramming strategy, obtaining patient-specific CiPSCs, which were differentiated into islet-like cells (CiPSC-islets) and injected underneath the abdominal anterior rectus sheath of the patient (red box indicates anatomical location).

(B) Timeline showing the patient's medical history, key time points of this study, as well as the workflow and quality controls during the manufacturing process of the patient-derived CiPSC-islets.

See also Figures S1, S2, and S3.

Based on assessments of panel reactive antibodies (PRAs), the patient was found to be PRA-positive for HLA-I and HLA-II antigens, indicating an increased risk of rejection and graft failure in the case of islet allotransplantation.[31–33] Therefore, in consultation with endocrinologists and transplant specialists, available treatment options were thoroughly discussed, including the option of enrolling in the TJFCH-iPS-001 study (ChiCTR2300072200) for autologous iPSC-derived islet transplantation. The patient was informed of the risks and benefits of this experimental therapy. Informed consent was signed, which stated potential risks and other treatment options. Following eligibility screening, the patient was enrolled as the first patient in the study. This report presents the 1-year endpoint results for the initial trial participant, providing data collected up to day 365 post-transplantation.

Generation of patient CiPSC-islets

Autologous CiPSCs were induced from adipose-derived mesenchymal stromal cells (ADSCs) isolated from the patient's adipose tissue by chemical reprogramming as described previously.[4] The procedures and QCs of this process are detailed in Methods S1 and Table S1, part 1. Systematic characterization of the selected patient CiPSC line used for downstream manufacture (patient CiPSC-#8) was performed, including trilineage differentiation potential and genomic stability assays.

The patient-specific CiPSC-islet cells were generated by subjecting patient CiPSC-#8 to six-stage stepwise directed differentiation using our previously established protocol.[20] The procedures and QCs were detailed in the patient CiPSC-islet differentiation workflow (Methods S1). Patient CiPSC-islets presented islet-sized aggregates containing approximately 60% β cells, 10% α-like cells, and 10% δ-like cells on average (Figures S1A–S1C). This was consistent with single-cell RNA sequencing (scRNA-seq) analysis of the patient CiPSC-islets, which also showed ∼13% endocrine progenitor cells and ∼8% enterochromaffin-like cells (Figures S1D–S1F) and similar global gene expression profiles of CiPSC-differentiated pancreatic endocrine cells to their native counterparts (Figures S1G and S1H).

Prior to the clinical study, the patient CiPSC-islets were assessed in 244 immunodeficient mice in transplantation experiments, with no tumorigenesis observed in all transplanted mice (Table S2). These transplantation experiments showed good survival of patient CiPSC-islets and an absence of teratoma formation or graft overgrowth (Figures S2A and S2B), including mice observed for an extended period of up to 58 weeks; by contrast, teratoma formation in CiPSC-#8-transplanted positive control mice rapidly resulted in teratoma formation (Figure S2C). Among them, 50 mice transplanted with the patient's CiPSC-islets underwent histopathological analysis of major organs (heart, liver, spleen, kidney, lung, and brain) at the end of the observation period (Figure S2D), showing absence of graft-related malignancy even in high-dose transplantation experiments of up to 1×10^7 per mouse (Table S2). In addition to safety evaluations in mice, the patient's CiPSC-islets were evaluated in nonhuman primates in a clinically relevant setting using the same transplantation strategy as that used in the patient of this study (i.e., implantation underneath the anterior abdominal rectus sheath), detailed in our previous study.[21] Four transplanted monkeys were assessed at 13 weeks post-transplantation by systemic ultrasonography and full autopsies, which showed no evidence of teratoma formation or abnormalities at any major organs.[21]

The *in vivo* potency of patient CiPSC-islets was also evaluated on a routinely used immunodeficient diabetic mouse model (Table S2). Patient CiPSC-islets consistently reversed diabetes in mice (Figures S2E and S2F; Table S2). The transplanted mice also showed restoration of glucose tolerance and glucose-responsive C-peptide secretion (Figures S2G and S2H). Mice transplanted with the patient's CiPSC-islets showed increased human C-peptide secretion to approximately 500 pmol/L, which was sustained thereafter for the observation period of 44 weeks (Figure S2I).

The patient CiPSC-islet manufacturing process was subject to in-process QCs as shown in Table S1, part 2. In particular, detection of potential residual PSCs, a source of tumorigenic risk, was conducted by digital droplet PCR (dd-PCR) analysis,[34] which showed no detectable residual PSCs in the CiPSC-islets (Table S1, part 4). Furthermore, whole genome/exome sequencing (WGS/WES) analyses showed no *de novo* genomic aberrations suggestive of tumorigenicity or pathogenicity in patient CiPSC-#8 or patient CiPSC-islets (Table S1, part 5). These findings demonstrated that the patient CiPSC-islets met the finalstage QC criteria. Dissociated patient-derived CiPSC-islet cells were cryopreserved for storage until transport to the clinical site.

Pre-transplant release of CiPSC-islets

3 days prior to the scheduled transplantation day, cryopreserved patient-derived CiPSC-islet cells were recovered and re-aggregated overnight. The CiPSC-islet aggregates were then collected and cultured for two more days, during which time final QC assessments were performed (Table S1, part 3). The CiPSC-islet preparation met release criteria for transplantation, presenting uniform spheroids between 50–250 μm and scarlet dithizone staining (Figures S3A and S3B), a high viability of 98% (Figure S3C; Table S1, part 3), and a Chromogranin A (CHGA)-positive proportion of 94.5% of total cells (Figures S3D and S3E), of which 56.4% were C-peptide and NKX6.1-positive cells. The CiPSC-islet preparation also contained 13.4% glucagon-positive cells and 15.9% somatostatin-positive cells, as determined by flow cytometry and immunofluorescence staining (Figures S3D–S3J). The CiPSC-islets were found to be glucose-responsive *in vitro*, with a glucose stimulation index of 1.37 (Table S1, part 3).

Transplantation of autologous CiPSC-islets

Considering the possibility of T1D autoimmunity relapse,[35,36] which might lead to islet graft injury and may potentially promote the development of alloimmune responses,[37] induction therapy was used. This consisted of basiliximab (20 mg on days 0 and 4) and etanercept (50 mg on day 0 and 25 mg on days 3, 7, and 10). As aforementioned, the patient had an existing transplanted liver, and the immunosuppressive maintenance regimen included tacrolimus, mycophenolate mofetil, and methylprednisolone tablets, which were continued after CiPSC transplantation (immunosuppressive regimen detailed in STAR Methods).

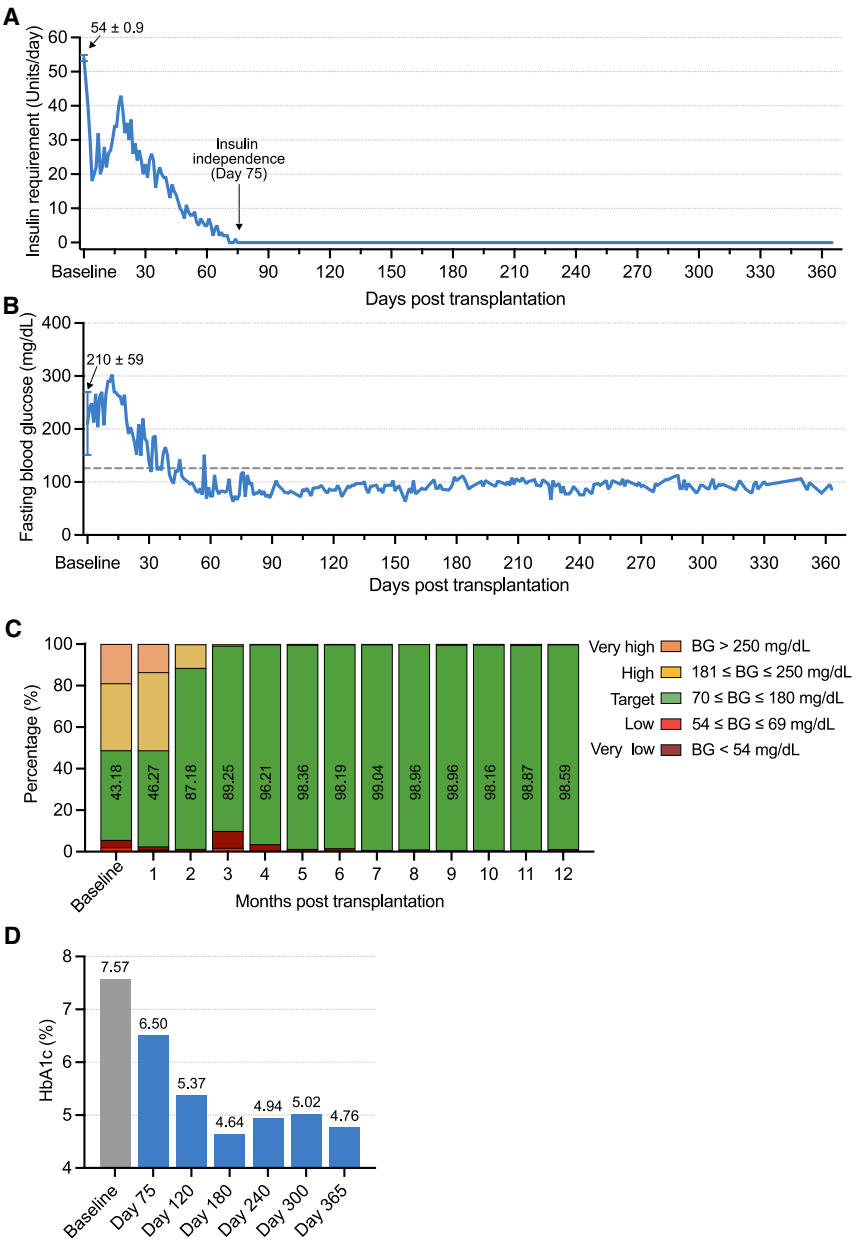

Figure 2. Exogenous insulin requirement and glycemic control pre- and post-transplantation of CiPSC-islets

(A) Exogenous insulin requirement pre- and post-transplantation of CiPSC-islets. The insulin dose pre-transplantation was 54 ± 0.9 units/day (mean ± SD). The arrow on day 75 indicates the starting day of complete insulin independence.

(B) Fasting blood glucose (FBG) levels pre- and post-transplantation of CiPSC-islets. The FBG before transplantation was 210 ± 59 mg/dL (mean ± SD). The dashed line at 126 mg/dL indicates the threshold for diabetes diagnosis as specified by ADA recommendations.[38]

(C) Proportion of time spent in the five glycemic ranges (very high, high, target, low, and very low, as specified by the ADA professional practice committee[29]) measured by CGM, before transplantation (baseline) and after transplantation. Percentages of time-in-target glycemic range (TIR) are indicated in the green bars. The baseline data were calculated using the data spanning 3 months before transplantation. BG, blood glucose.

(D) HbA1c levels pre-transplantation (baseline) and on post-transplantation follow-up visits. The patient's HbA1c was slightly lower than anticipated for her TIR, a variation that has been reported for patients with chronic liver disease.[39–41]

CiPSC-islets were administered to the patient by injection underneath the abdominal anterior rectus sheath at a dose of 19,843 islet equivalent (IEQ)/kg (a total of 1,488,283 IEQ) under the guidance of ultrasound on June 25th, 2023 (Figure S4A).

Glycemic control

Within 2 weeks after transplantation, the patient's daily exogenous insulin dose requirement began to reduce from baseline of 54 ± 0.9 units/day (Figure 2A). From day 18 post-transplantation, the patient's daily insulin dose requirement decreased steadily from 43 units/day. The patient achieved complete insulin independence on day 75. Thereafter, the patient remained insulin-independent for the follow-up period of 1 year (Figure 2A).

The patient's glycemic control was evaluated by CGM and HbA1c levels. The patient's fasting blood glucose (FBG) monitored by CGM was 210 ± 59 (mean ± SD) mg/dL during the three months before transplantation (Figure 2B). After transplantation, the FBG gradually decreased. Following the achievement of insulin independence, the patient's FBG was maintained below the threshold for diabetes diagnosis (126 mg/dL[38]) (Figure 2B).

The CGM data demonstrated that the patient achieved substantial improvement in blood glucose time-in-range (TIR) in comparison with baseline measurements (Figure 2C). TIR represents time spent within a target blood glucose range (typically 70–180 mg/dL), and the ADA recommended TIR target for patients with T1D is 70%. A TIR of 87.18% was achieved in the patient at month 2 post-transplantation, which increased to 96.21% at month 4 (Figure 2C). An increase in time below the target range (TBR) was observed during the period of insulin discontinuation (weeks 10–11 in month 3, gradually alleviated 2 weeks later). At the 1-year endpoint, the patient's TIR had been >98% for 8 months, a substantial improvement in comparison with the baseline TIR of 43.18% (Figure 2C).

Concordant with the improved FBG and TIR, the patient's HbA1c value showed a reduction from 7.57% at baseline to 6.50% at the day 75 visit (Figure 2D), aligning with the lower limit of the recommended HbA1c standard for diabetes diagnosis.[38] At the day 120 visit, the patient's HbA1c value decreased to

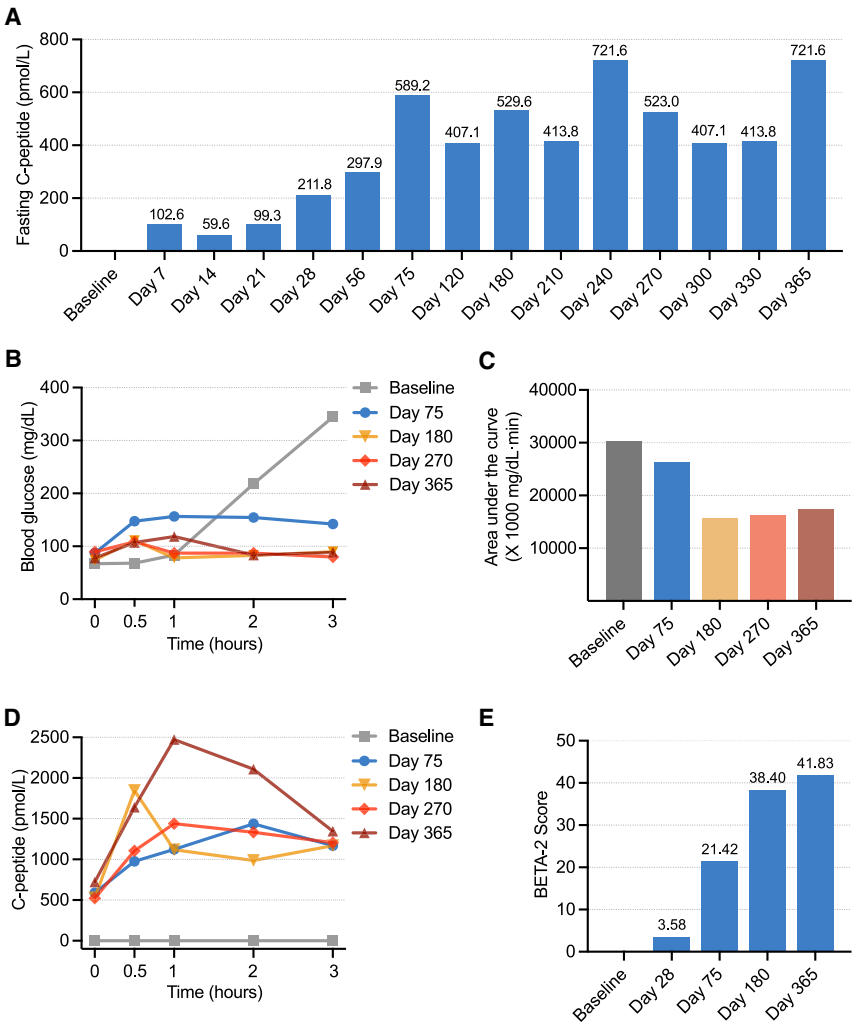

Figure 3. Evaluation of CiPSC-islet graft function

(A) Fasting C-peptide levels pre-transplantation (baseline) and on post-transplantation follow-up visits.

(B) Blood glucose during 3 h oral glucose tolerance test (OGTT) pre-transplantation (baseline, gray) and on post-transplantation follow-up visits on days 75, 180, 270, and 365.

(C) Area under the curve of glucose levels during the OGTT from (B).

(D) C-peptide levels during the OGTT in (B). The values of fasting C-peptide levels at the 0-h mark also appear in (A) as the values of follow-up visits days 75, 180, 270, and 365.

(E) BETA-2 score calculated at pre-transplantation (baseline) and on post-transplantation follow-up visits.

See also Figure S4.

5.37% and was maintained in the non-diabetic range (<5.7%)[38] thereafter (Figure 2D), achieving the primary study endpoint of HbA1c <7% from 90–365 days post-transplantation. The improvements in FBG, TIR, and HbA1c and the achievement of insulin independence demonstrated a restoration of the patient's glycemic control following CiPSC-islet transplantation.

Graft function

After CiPSC-islet transplantation, the patient's fasting serum C-peptide level, which was undetectable at baseline, increased promptly and reached levels ranging 59.6–102.6 pmol/L by the second week after transplantation (Figure 3A). From the day 28 visit, the patient's fasting C-peptide level increased further. After insulin independence, the fasting C-peptide reached a plateau and fluctuated within a range of 407.1 to 721.6 pmol/L. Notably, meal-responsiveness was detected on the day 56 visit, when C-peptide secretion increased by 20% at 2 h post-meal (350.9 vs. 297.9 pmol/L) (Figure S4B). At the day 120 visit, the meal-responsiveness of C-peptide secretions was further improved, with a fasting level of 407.1 pmol/L and a 2-h post-prandial level of 834.1 pmol/L.

During the oral glucose-tolerance test (OGTT) before transplantation, the patient's blood glucose level surged from 67 mg/dL at 0 h to 344 mg/dL at the final measure taken at 3 h after glucose administration (Figure 3B). C-peptide measures taken in parallel showed undetectable C-peptide levels (Figure 3D), indicating a complete destruction of β cells and poor glucose tolerance. By contrast, at the day 75 visit after transplantation, the patient's blood glucose level remained relatively stable during OGTT (Figure 3B). The blood glucose measurement at the 2 h time point was 155 mg/dL, which is below the diagnostic threshold for diabetes (≥200 mg/dL at 2 h).[38] The area under the curve was also markedly decreased (Figure 3C). The parallel C-peptide levels were 589.2 pmol/L in the fasting state and peaked at 2 h after glucose administration at 1,436.5 pmol/L, showing a 2.4-fold stimulation (Figure 3D).

From the day 180 visit, the patient's glucose tolerance showed further improvement, showing relatively stable performance in OGTTs of subsequent visits thereafter (Figures 3B and 3D). The blood glucose levels at the 2 h mark were consistently between 83–87 mg/dL, falling within the normal range of <140 mg/dL[38] (Figure 3B). The area under the curve further decreased and remained stable (Figure 3C). OGTT tests on days 180, 270, and 365 visits showed peak C-peptide levels of 1,847.0, 1,439.9, and 2,472.6 pmol/L, respectively, while the fold change in peak C-peptide values relative to the fasting C-peptide values was 3.5, 2.8, and 3.4, respectively (Figure 3D). These data indicated more potent insulin secretion by the graft in response to oral glucose administration since the day 180 visit compared with day 75.

The BETA-2 score is a composite metric predicting β cell function as well as treatment outcomes of islet transplantation.[42–45] The patient's BETA-2 score increased steadily from a baseline

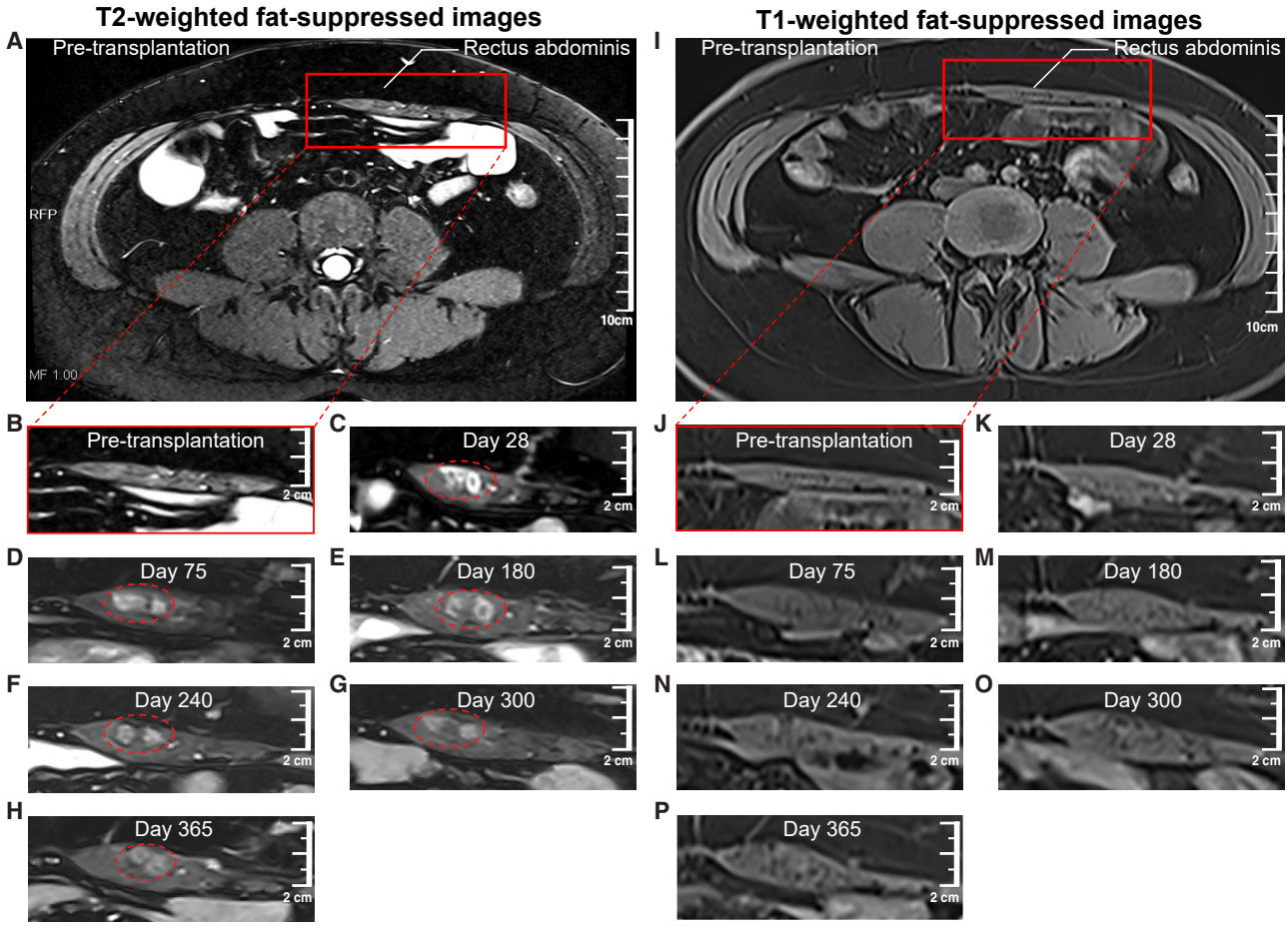

Q

Tumor biomarkers

	Normal range	Pre-Transplantation	Day 28	Day 75	Day 180	Day 240	Day 300	Day 365
β-HCG (mIU/mL)	**0-5.30**	< 0.10	n.d.	n.d.	< 0.10	< 0.10	< 0.10	< 0.10
AFP (ng/mL)	**0-7.00**	1.58	1.90	1.57	1.38	1.81	1.14	1.76
CEA (ng/mL)	**0-5.00**	1.25	1.31	1.63	0.94	1.22	1.32	1.42
CA125 (ng/mL)	**0-47.00**	17.60	17.00	15.10	11.70	11.20	10.30	11.90
CA15-3 (ng/mL)	**0-24.00**	12.80	10.90	10.20	9.31	9.24	9.92	10.10
CA19-9 (ng/mL)	**0-30.00**	28.90	30.00	21.30	21.00	19.70	19.00	21.70

Figure 4. MRI images of the CiPSC-islet graft site beneath the abdominal rectus sheath

Axial T2-weighted fat-suppressed (T2W-FS) (A–H) and T1-weighted fat-suppressed (T1W-FS) images (I–P) pre-transplantation and on post-transplantation follow-up visits of Days 28, 75, 180, 240, 300, and 365. T2W-FS imaging highlights the morphology of the graft, and T1W-FS imaging showed no abnormal fat deposition, which is associated with teratoma formation.[46]

(A–H) T2W-FS images of the left rectus abdominis before transplantation (A and B) and after transplantation (C–H), which showed patchy and small nodular-like high-signal areas, indicating the location of transplanted CiPSC-islets. During regular monitoring within 365 days after transplantation, this signal remained stable in terms of location, shape, size, and MR signal intensity.

(legend continued on next page)

value of 0.13 to 21.42 by the day 75 visit, with the most recent value of 41.83 at day 365 visit (Figure 3E), indicating successful engraftment of CiPSC-islets in the subanterior rectus sheath. Taken together, these results indicated good graft function of the transplanted CiPSC-islets and recovery of endogenous, glucose-responsive insulin secretion in the patient.

Safety assessments

The transplantation beneath the abdominal anterior rectus sheath offers advantages for convenient monitoring of the implanted CiPSC-islets using ultrasound and magnetic resonance imaging (MRI) techniques. The site was visualized by ultrasound before, during, and 3 days post-transplantation, which showed CiPSC-islets localized between the anterior rectus sheath and the rectus abdominis (Figure S4A).

We used MRI to regularly monitor the graft and the transplantation site, focusing on the detection of any abnormal growth. The T2-weighted fat-suppressed (T2W-FS) imaging facilitates visualization of any morphological changes at the transplantation site, the left rectus abdominis (Figures 4A–4H). T2W-FS images taken on day 28 post-transplantation revealed patchy, small, nodular high-signal areas at the left rectus abdominis (Figure 4C), compared with the images obtained before transplantation (Figures 4A and 4B), indicating the location of the transplanted CiPSC-islet grafts. Subsequent T2W-FS images taken over the following 365 days after transplantation showed that the signal of the grafts remained consistent and stable in terms of location, shape, size, and magnetic resonance signal intensity, and the left abdominal rectus exhibited no signs of compression, displacement, or deformation, which together showed no indication of abnormal growth (Figures 4D–4H). The T1W-FS imaging was used to detect abnormalities such as abnormal fat accumulation, which is a feature of teratoma.[46] In this patient, the transplantation area exhibited signal intensities comparable to the surrounding normal muscle tissue (iso-signal), indicating absence of abnormal fat accumulation (Figures 4I–4P). Taken together, both T2W-FS and T1W-FS images indicated no evidence of teratoma formation in the graft site during the 1-year follow-up.

In this study, the typical serum markers for teratoma—beta-human chorionic gonadotropin (β-HCG), alpha fetoprotein (AFP), and carcinoembryonic antigen (CEA)[47–49]—were monitored before and after transplantation, together with other tumor biomarkers, carbohydrate antigen 125 (CA125), cancer antigen 15–3 (CA15-3), and carbohydrate antigen 199 (CA19-9). We consistently observed that all the measures were in the normal range (Figure 4Q). No signs of teratoma were detected by the medical imaging or tumor marker measures throughout the 1-year follow-up.

Diabetes autoantibodies were monitored both before and after the transplantation (Table S3). Insulin autoantibody (IAA), islet cell antibody (ICA), insulinoma-associated-2 antibodies (IA-2Ab), and zinc transporter 8 antibody (ZnT8) were consistently indicated as negative. A slight elevation in glutamic acid decarboxylase antibody (GADA) level at one time point was observed.

All adverse events (AEs) and severe AEs (SAEs) throughout the 1-year follow-up period were recorded and listed in Table 1. The treatment-emergent AEs were limited to the peri-transplantation period, which included pain at the puncture area and nausea and vomiting due to general anesthesia. No treatment-emergent SAEs were observed. Throughout follow-up, the patient was hospitalized one time for an upper respiratory tract infection and was discharged 5 days later. No occurrence of severe hypoglycemic events was observed throughout follow-up.

DISCUSSION

We report here autologous transplantation of CiPSC-islets in a patient with T1D. Before transplantation, the patient suffered from long-term, hard-to-control diabetes complicated by episodes of severe hypoglycemia. After CiPSC-islet transplantation, the patient achieved insulin independence within 3 months post-transplantation, ultimately achieving over 98% blood glucose TIR without exogenous insulin use. These findings supported the viability of CiPSC-islet transplantation underneath the abdominal anterior rectus sheath, which led to relatively rapid restoration of insulin-independent glycemic control in the patient.

Insulin independence and glycemic control

This report demonstrates attainment of insulin-independent glycemic control in the patient, as seen by a blood glucose TIR of over 98% after month 4 post-transplantation and decrease in HbA1c to a non-diabetic level. Studies have shown that increased TIR reduces the hazard ratio for complications,[50,51] while each 1% reduction of HbA1c toward the physiological level has been associated with a 21% reduction in risk of diabetes-related complications and death.[52] According to recent reports, only approximately 25% of patients with T1D meet the ADA-recommended HbA1c target of 7.0% on exogenous insulin treatment.[53–56] Importantly, a crucial clinical benefit of islet transplantation is the protection from severe hypoglycemic events, which is a predominantly life-threatening condition and a source of fear and distress in T1D patients.[57,58] No occurrence of severe hypoglycemic events was observed throughout 1-year follow-up after CiPSC-islet transplantation. Taken together, the findings suggest a positive impact on the metabolic outcomes of the patient using this treatment approach.

Transplantation strategy

This report describes for the first time the use of stem-cell-derived islet transplantation underneath the abdominal anterior

(I–P) T1W-FS images of the left rectus abdominis before transplantation (I and J) and after transplantation (K–P), which showed comparable signal intensities at the graft location in the patient's left rectus abdominis to the surrounding normal muscle (iso-signal). Scale bar for (A) and (I): 10 cm; scale bar for (B)–(H) and (J)–(P): 2 cm.

(Q) Measurements of tumor biomarkers in patient venous blood samples pre-transplantation and on post-transplantation follow-up visits. β-HCG, beta-human chorionic gonadotropin; AFP, alpha fetoprotein; CEA, carcinoembryonic antigen; CA125, carbohydrate antigen 125; CA15-3, cancer antigen 15-3; CA19-9, carbohydrate antigen 19-9; n.d., not detected.

See also Figure S4.

Table 1. Adverse events

AEs[a]	Date of onset	Expression site	SAEs[b]	Treatment	Outcome	Recovery date	Causality between AEs and the protocol
Pain at the puncture area	2023/06/25	implantation site	no	none	recovered	2023/06/25	yes (implantation-procedure-related)
Nausea and vomiting	2023/06/27	outside the implantation site	no	symptomatic treatment	recovered	2023/06/27	yes (general-anesthesia-related)
Sore throat and nasal congestion	2023/09/14	outside the implantation site	no	none	recovered	2023/09/15	no
Upper respiratory tract infection	2023/11/30	outside the implantation site	yes	symptomatic treatment	recovered	2023/12/05	no

[a]AEs, adverse events.
[b]SAEs, serious adverse events.

rectus sheath in human. Alternative islet transplantation sites have been reported over the years, including the omentum[27] and intramuscular site in the forearm[25]; however, clear improvements over the conventional intraportal site have not been well demonstrated.[59] The positive metabolic data seen in this clinical study are consistent with that seen in our preclinical study in nonhuman primates, in which we sought to identify an optimal transplant site for CiPSC-islets.[21] We compared the transplantation of hPSC-islets underneath the abdominal anterior rectus sheath and an intramuscular and subcutaneous site in nonhuman primates and found the anterior rectus sheath to be beneficial in supporting the engraftment, vascularization, and functional maturation of the PSC-islets, resulting in markedly increased C-peptide secretion when compared with intrahepatic transplantation.[20,21] Other important advantages of this transplant site include the circumvention of graft loss from IBMIR.[22,24] These findings suggest that the favorable engraftment microenvironment at this site may be an underlying factor to the robust C-peptide secretion and relatively rapid reversal of diabetes observed in the patient.

Data from another clinical trial (NCT04786262), which transplanted hPSC-derived islets into the hepatic portal vein, were recently announced, the findings of which also indicated positive outcomes post-transplantation.[60] In this study, an extrahepatic site was employed, which was a favorable option for this patient on account of her transplanted liver. In comparison to intraportal transplantation, the abdominal rectus sheath site also encompasses other safety considerations, such as ease of access for transplantation and imaging and site retention of graft.[21] After CiPSC-islet transplantation into the patient, we demonstrate that the graft could be routinely imaged by ultrasound and MRI as necessary for regular detection of morphological changes at the site. The possibility for routine safety monitoring at this transplant site is an important step forward that is critical to exploratory stem-cell-based cellular therapies. Importantly, transplantation to this site supports graft retrieval if necessary. Taken together with our preclinical studies, the clinical data in this report support the clinical value of this transplantation strategy, warranting continued exploration.

Autologous chemically induced stem-cell-derived islets

The patient in this study suffered from hard-to-control diabetes despite intensive insulin treatment. To improve glycemic control, the patient had previously received a pancreas transplantation in 2017, which had to be removed a year later due to thrombotic complications. However, on account of her PRA-positive status, an allogeneic pancreas or islet transplant would be at high risk for rejection,[31–33] making the opportunity for an autologous transplant for this patient a valuable treatment option.

CiPSCs possess characteristics that are potentially advantageous to the clinical manufacture of autologous stem cells. The small molecules used in the chemical reprogramming approach offer ease of manufacture and standardization and are highly controllable, scalable, and cost-effective, which are important for standardized manufacturing of therapeutic cells.[6] In addition, potential benefits of CiPSCs in comparison to transcription factor-reprogrammed iPSCs have been demonstrated in studies analyzing mouse CiPSCs, which demonstrated potential improvements in genomic stability and closer epigenetic features to ESCs.[61–64] While further evaluation is required, these findings suggest potential advantages of CiPSCs for clinical applications.

In this study, good-manufacturing-practice-compliant manufacture of personalized CiPSC-islets for autologous transplantation was conducted, allowing for the first report of clinical transplantation of CiPSC-derived cells. Taken together, these findings indicate the feasibility of chemically induced autologous PSCs for cell therapy, constituting a viable personalized medicine strategy.

Limitations of the study

A few limitations exist in this study. Firstly, safety and efficacy beyond 1 year and in more patients remain to be evaluated. The trial is ongoing and includes three patients in total. After interim analysis of the first patient and the submission of this work, the second and third patients were enrolled. Follow-up with these patients is ongoing, as they were sequentially enrolled in accordance with regulatory safety requirements. However, due to the limited follow-up period and according to our clinical trial protocol, data from these two patients are not yet matured for reporting. Regardless, given the relatively small size of the cohort in this phase I clinical trial, further study in a larger cohort of patients is warranted. Secondly, the use of immunosuppressants in this patient precluded the evaluation of immune response of the recipient to the autologous graft. Because T1D is an autoimmune disease, an autologous islet transplant would

likely still necessitate the use of immunosuppressants. However, this patient was already on immunosuppressants for a transplanted liver, and this allowed the assessment of therapeutic capacity of CiPSC-islets without adding to the patient's immunosuppression burden, but insight into potential autoimmune response was limited.

Taken together, this study reports positive clinical data in this patient after CiPSC-islet transplantation, as well as the realization of routine, non-invasive graft monitoring underneath the abdominal anterior rectus sheath. Overall, the findings support further clinical studies in this direction and mark a step forward in achieving the potential of personalized cell therapy using CiPSCs to treat disease.

RESOURCE AVAILABILITY

Lead contact

Further information and requests for resources should be directed to and will be fulfilled by the lead contact, hongkui_deng@pku.edu.cn.

Materials availability

This study did not generate new reagents.

Data and code availability

- Single-cell RNA-seq and WGS/WES data have been deposited at the Genome Sequence Archive of the National Genomics Data Center and are publicly available as of the date of publication. Accession numbers are GSA for Human: HRA006309 and GSA for Human: HRA007623, respectively.
- This paper does not report original code.
- Any additional information required to reanalyze the data reported in this paper is available from the lead contact upon request.

ACKNOWLEDGMENTS

This work is supported by the National Key Research and Development Program of China (2020YFA0803704), the National Natural Science Foundation of China (32288102, 82070805, and 82100841), the Foundation by Institute of Transplantation Medicine Nankai University (no. NKTM2023002), the Tianjin Municipal Human Resources and Social Security Bureau (XB202011), the Tianjin Municipal Science and Technology Bureau (22JCZXJC00110), and the "Pioneer" and "Leading Goose" R&D Program of Zhejiang, China (2023C03019). The authors would like to thank Jun Xu, Bei Liu, Jinlin Wang, Yulin Liu, Shicheng Sun, and Jingyang Guan for discussions and critique of the manuscript. We thank Zhen Liang for early contributions to development of the transplantation strategy. The authors thank Mingzhe Han, Deling Kong, Hong Zheng, Chao Sun, Xia Jiang, and Junfeng Li for guidance on clinical investigation. We would also like to thank Shuli Zhi for support on single-cell sequencing and Yulin Lv and Shanshan Xiao for support with single-cell analysis.

AUTHOR CONTRIBUTIONS

H.D., Z.S., and Shusen Wang conceived of and designed the clinical study. Planning and conceptualization were performed by H.D., the lead scientist of the study. Clinical investigation was conducted by Shusen Wang, Z.S., B.Z., Z.L., X.C., W.G., Xuelian Wang, X.D., Y.Z., and Y. Weng. Transplantation surgery was performed by Shusen Wang, B.Z., Z.L., and M.W. Ultrasound was performed by M.W. Preclinical experiments were performed by Y.D., G.M., S.Y.L., Z.Z., Xiaofeng Wang, and J.G. Cell manufacturing was performed by S. Wu, T. Liang, and Y. Wei. Cell manufacturing quality controls were performed by S. Wu and D.Z. Pre-transplantation quality controls were performed by R.L., J.Z., T. Liu, N.L., X.D., P.S., J.Y., C.Z., Z.W., and H.H. Early trial application processes were conducted by Y.D., Shusen Wang, and Z.L. Analysis and interpretation of data were performed by Shusen Wang, G.M., S.Y.L., and R.L. H.D., Shusen Wang, S.Y.L., G.M., R.L., and Y.D. wrote and revised the manuscript. Imaging examination and analyses were performed by X.S. Procurement of patient adipose tissue was performed by Shuang Wang. dd-PCR testing was established and performed by Y.P.

DECLARATION OF INTERESTS

H.D. is a scientific advisor at Hangzhou Reprogenix Bioscience. G.M. and S.L. are employees of Hangzhou Reprogenix Bioscience. Y.D. is a former employee of Hangzhou Reprogenix Bioscience and is now affiliated with the Hangzhou Institute of Medicine, Chinese Academy of Sciences. H.D., Y.D., G.M., and Z.Z. have patent applications related to this work.

STAR★METHODS

Detailed methods are provided in the online version of this paper and include the following:

- KEY RESOURCES TABLE
- EXPERIMENTAL MODEL AND STUDY PARTICIPANT DETAILS
- METHOD DETAILS
  - Generation of CiPSCs from the patient's adipose-derived mesenchymal stromal cells
  - Assessment of patient CiPSC clones
  - Preparation of CiPSC-islets and safety assessment
  - Whole genome/exome sequencing (WGS/WES)
  - Single cell RNA-sequencing analysis
  - Short-tandem repeat (STR) analysis
  - Immunofluorescence
  - Teratoma formation
  - RT–qPCR analysis
  - Transplantation in mouse model
  - Flow cytometry
  - Glucose stimulated insulin secretion (GSIS) assay
  - Cell preparation and subanterior rectus sheath transplantation
  - Immunosuppression and other medications
  - Laboratory methods
- QUANTIFICATION AND STATISTICAL ANALYSIS
  - BETA-2 score calculation
- ADDITIONAL RESOURCES

SUPPLEMENTAL INFORMATION

Supplemental information can be found online at https://doi.org/10.1016/j.cell.2024.09.004.

Received: October 3, 2023
Revised: June 25, 2024
Accepted: September 4, 2024
Published: September 25, 2024

REFERENCES

1. Shi, Y., Inoue, H., Wu, J.C., and Yamanaka, S. (2017). Induced pluripotent stem cell technology: a decade of progress. Nat. Rev. Drug Discov. *16*, 115–130. https://doi.org/10.1038/nrd.2016.245.
2. Takahashi, K., Tanabe, K., Ohnuki, M., Narita, M., Ichisaka, T., Tomoda, K., and Yamanaka, S. (2007). Induction of pluripotent stem cells from adult human fibroblasts by defined factors. Cell *131*, 861–872. https://doi.org/10.1016/j.cell.2007.11.019.
3. Yu, J., Vodyanik, M.A., Smuga-Otto, K., Antosiewicz-Bourget, J., Frane, J.L., Tian, S., Nie, J., Jonsdottir, G.A., Ruotti, V., Stewart, R., et al. (2007). Induced pluripotent stem cell lines derived from human somatic cells. Science *318*, 1917–1920. https://doi.org/10.1126/science.1151526.
4. Guan, J., Wang, G., Wang, J., Zhang, Z., Fu, Y., Cheng, L., Meng, G., Lyu, Y., Zhu, J., Li, Y., et al. (2022). Chemical reprogramming of human somatic

cells to pluripotent stem cells. Nature *605*, 325–331. https://doi.org/10.1038/s41586-022-04593-5.

5. Liuyang, S., Wang, G., Wang, Y., He, H., Lyu, Y., Cheng, L., Yang, Z., Guan, J., Fu, Y., Zhu, J., et al. (2023). Highly efficient and rapid generation of human pluripotent stem cells by chemical reprogramming. Cell Stem Cell *30*, 450–459.e9. https://doi.org/10.1016/j.stem.2023.02.008.
6. Wang, J., Sun, S., and Deng, H. (2023). Chemical reprogramming for cell fate manipulation: Methods, applications, and perspectives. Cell Stem Cell *30*, 1130–1147. https://doi.org/10.1016/j.stem.2023.08.001.
7. Shi, Y., Hou, L., Tang, F., Jiang, W., Wang, P., Ding, M., and Deng, H. (2005). Inducing embryonic stem cells to differentiate into pancreatic beta cells by a novel three-step approach with activin A and all-trans retinoic acid. Stem Cells *23*, 656–662. https://doi.org/10.1634/stemcells.2004-0241.
8. D'Amour, K.A., Bang, A.G., Eliazer, S., Kelly, O.G., Agulnick, A.D., Smart, N.G., Moorman, M.A., Kroon, E., Carpenter, M.K., and Baetge, E.E. (2006). Production of pancreatic hormone-expressing endocrine cells from human embryonic stem cells. Nat. Biotechnol. *24*, 1392–1401. https://doi.org/10.1038/nbt1259.
9. Jiang, W., Shi, Y., Zhao, D., Chen, S., Yong, J., Zhang, J., Qing, T., Sun, X., Zhang, P., Ding, M., et al. (2007). In vitro derivation of functional insulin-producing cells from human embryonic stem cells. Cell Res. *17*, 333–344. https://doi.org/10.1038/cr.2007.28.
10. Kroon, E., Martinson, L.A., Kadoya, K., Bang, A.G., Kelly, O.G., Eliazer, S., Young, H., Richardson, M., Smart, N.G., Cunningham, J., et al. (2008). Pancreatic endoderm derived from human embryonic stem cells generates glucose-responsive insulin-secreting cells in vivo. Nat. Biotechnol. *26*, 443–452. https://doi.org/10.1038/nbt1393.
11. Tateishi, K., He, J., Taranova, O., Liang, G., D'Alessio, A.C., and Zhang, Y. (2008). Generation of insulin-secreting islet-like clusters from human skin fibroblasts. J. Biol. Chem. *283*, 31601–31607. https://doi.org/10.1074/jbc.M806597200.
12. Zhang, D., Jiang, W., Liu, M., Sui, X., Yin, X., Chen, S., Shi, Y., and Deng, H. (2009). Highly efficient differentiation of human ES cells and iPS cells into mature pancreatic insulin-producing cells. Cell Res. *19*, 429–438. https://doi.org/10.1038/cr.2009.28.
13. Pagliuca, F.W., Millman, J.R., Gürtler, M., Segel, M., Van Dervort, A., Ryu, J.H., Peterson, Q.P., Greiner, D., and Melton, D.A. (2014). Generation of functional human pancreatic beta cells in vitro. Cell *159*, 428–439. https://doi.org/10.1016/j.cell.2014.09.040.
14. Rezania, A., Bruin, J.E., Arora, P., Rubin, A., Batushansky, I., Asadi, A., O'Dwyer, S., Quiskamp, N., Mojibian, M., Albrecht, T., et al. (2014). Reversal of diabetes with insulin-producing cells derived in vitro from human pluripotent stem cells. Nat. Biotechnol. *32*, 1121–1133. https://doi.org/10.1038/nbt.3033.
15. Veres, A., Faust, A.L., Bushnell, H.L., Engquist, E.N., Kenty, J.H.R., Harb, G., Poh, Y.C., Sintov, E., Gürtler, M., Pagliuca, F.W., et al. (2019). Charting cellular identity during human in vitro beta-cell differentiation. Nature *569*, 368–373. https://doi.org/10.1038/s41586-019-1168-5.
16. Nair, G.G., Liu, J.S., Russ, H.A., Tran, S., Saxton, M.S., Chen, R., Juang, C., Li, M.L., Nguyen, V.Q., Giacometti, S., et al. (2019). Recapitulating endocrine cell clustering in culture promotes maturation of human stem-cell-derived beta cells. Nat. Cell Biol. *21*, 263–274. https://doi.org/10.1038/s41556-018-0271-4.
17. Alvarez-Dominguez, J.R., Donaghey, J., Rasouli, N., Kenty, J.H.R., Helman, A., Charlton, J., Straubhaar, J.R., Meissner, A., and Melton, D.A. (2020). Circadian Entrainment Triggers Maturation of Human In Vitro Islets. Cell Stem Cell *26*, 108–122.e10. https://doi.org/10.1016/j.stem.2019.11.011.
18. Hogrebe, N.J., Augsornworawat, P., Maxwell, K.G., Velazco-Cruz, L., and Millman, J.R. (2020). Targeting the cytoskeleton to direct pancreatic differentiation of human pluripotent stem cells. Nat. Biotechnol. *38*, 460–470. https://doi.org/10.1038/s41587-020-0430-6.
19. Liu, H., Yang, H., Zhu, D., Sui, X., Li, J., Liang, Z., Xu, L., Chen, Z., Yao, A., Zhang, L., et al. (2014). Systematically labeling developmental stage-specific genes for the study of pancreatic beta-cell differentiation from human embryonic stem cells. Cell Res. *24*, 1181–1200. https://doi.org/10.1038/cr.2014.118.
20. Du, Y., Liang, Z., Wang, S., Sun, D., Wang, X., Liew, S.Y., Lu, S., Wu, S., Jiang, Y., Wang, Y., et al. (2022). Human pluripotent stem-cell-derived islets ameliorate diabetes in non-human primates. Nat. Med. *28*, 272–282. https://doi.org/10.1038/s41591-021-01645-7.
21. Liang, Z., Sun, D., Lu, S., Lei, Z., Wang, S., Luo, Z., Zhan, J., Wu, S., Jiang, Y., Lu, Z., et al. (2023). Implantation underneath the abdominal anterior rectus sheath enables effective and functional engraftment of stem-cell-derived islets. Nat. Metab. *5*, 29–40. https://doi.org/10.1038/s42255-022-00713-7.
22. Mehigan, D.G., Bell, W.R., Zuidema, G.D., Eggleston, J.C., and Cameron, J.L. (1980). Disseminated intravascular coagulation and portal hypertension following pancreatic islet autotransplantation. Ann. Surg. *191*, 287–293. https://doi.org/10.1097/00000658-198003000-00006.
23. Shapiro, A.M., Lakey, J.R., Ryan, E.A., Korbutt, G.S., Toth, E., Warnock, G.L., Kneteman, N.M., and Rajotte, R.V. (2000). Islet transplantation in seven patients with type 1 diabetes mellitus using a glucocorticoid-free immunosuppressive regimen. N. Engl. J. Med. *343*, 230–238. https://doi.org/10.1056/NEJM200007273430401.
24. Moberg, L., Johansson, H., Lukinius, A., Berne, C., Foss, A., Källen, R., Østraat, Ø., Salmela, K., Tibell, A., Tufveson, G., et al. (2002). Production of tissue factor by pancreatic islet cells as a trigger of detrimental thrombotic reactions in clinical islet transplantation. Lancet *360*, 2039–2045. https://doi.org/10.1016/s0140-6736(02)12020-4.
25. Rafael, E., Tibell, A., Rydén, M., Lundgren, T., Sävendahl, L., Borgström, B., Arnelo, U., Isaksson, B., Nilsson, B., Korsgren, O., and Permert, J. (2008). Intramuscular autotransplantation of pancreatic islets in a 7-year-old child: a 2-year follow-up. Am. J. Transplant *8*, 458–462.
26. Maffi, P., Balzano, G., Ponzoni, M., Nano, R., Sordi, V., Melzi, R., Mercalli, A., Scavini, M., Esposito, A., Peccatori, J., et al. (2013). Autologous pancreatic islet transplantation in human bone marrow. Diabetes *62*, 3523–3531. https://doi.org/10.2337/db13-0465.
27. Baidal, D.A., Ricordi, C., Berman, D.M., Alvarez, A., Padilla, N., Ciancio, G., Linetsky, E., Pileggi, A., and Alejandro, R. (2017). Bioengineering of an Intraabdominal Endocrine Pancreas. N. Engl. J. Med. *376*, 1887–1889. https://doi.org/10.1056/NEJMc1613959.
28. Wszola, M., Berman, A., Gorski, L., Ostaszewska, A., Serwanska-Swietek, M., Krajewska, M., Lipinska, A., Chmura, A., and Kwiatkowski, A. (2018). Endoscopic Islet Autotransplantation Into Gastric Submucosa-1000-Day Follow-up of Patients. Transplant. Proc. *50*, 2119–2123. https://doi.org/10.1016/j.transproceed.2018.02.138.
29. American Diabetes Association Professional; Practice Committee (2024). 6. Glycemic Goals and Hypoglycemia: Standards of Care in Diabetes-2024. Diabetes Care *47*, S111–S125. https://doi.org/10.2337/dc24-S006.
30. Shapiro, A.M.J., Pokrywczynska, M., and Ricordi, C. (2017). Clinical pancreatic islet transplantation. Nat. Rev. Endocrinol. *13*, 268–277. https://doi.org/10.1038/nrendo.2016.178.
31. Mohanakumar, T., Narayanan, K., Desai, N., Ramachandran, S., Shenoy, S., Jendrisak, M., Susskind, B.M., Olack, B., Benshoff, N., Phelan, D.L., et al. (2006). A significant role for histocompatibility in human islet transplantation. Transplantation *82*, 180–187. https://doi.org/10.1097/01.tp.0000226161.82581.b2.
32. Campbell, P.M., Senior, P.A., Salam, A., Labranche, K., Bigam, D.L., Kneteman, N.M., Imes, S., Halpin, A., Ryan, E.A., and Shapiro, A.M. (2007). High risk of sensitization after failed islet transplantation. Am. J. Transplant *7*, 2311–2317. https://doi.org/10.1111/j.1600-6143.2007.01923.x.
33. Campbell, P.M., Salam, A., Ryan, E.A., Senior, P., Paty, B.W., Bigam, D., McCready, T., Halpin, A., Imes, S., Al Saif, F., et al. (2007). Pretransplant HLA antibodies are associated with reduced graft survival after clinical

islet transplantation. Am. J. Transplant *7*, 1242–1248. https://doi.org/10.1111/j.1600-6143.2007.01777.x.

34. Wu, Y., Zhang, Z., Wu, S., Chen, Z., and Pu, Y. (2023). Estimating residual undifferentiated cells in human chemically induced pluripotent stem cell derived islets using lncRNA as biomarkers. Sci. Rep. *13*, 16435. https://doi.org/10.1038/s41598-023-43798-0.
35. Stegall, M.D., Lafferty, K.J., Kam, I., and Gill, R.G. (1996). Evidence of recurrent autoimmunity in human allogeneic islet transplantation. Transplantation *61*, 1272–1274. https://doi.org/10.1097/00007890-199604270-00027.
36. Worcester; Human; Islet; Transplantation Group, Sharma, V., Andersen, D., Thompson, M., Woda, B.A., Stoff, J.S., Hartigan, C., Rastellini, C., Phillips, D., Mordes, J.P., et al. (2006). Autoimmunity after islet-cell allotransplantation. N. Engl. J. Med. *355*, 1397–1399. https://doi.org/10.1056/NEJMc061530.
37. Subramanian, V., and Mohanakumar, T. (2012). Chronic rejection: a significant role for Th17-mediated autoimmune responses to self-antigens. Expert Rev. Clin. Immunol. *8*, 663–672.
38. American Diabetes Association Professional; Practice Committee (2024). 2. Diagnosis and Classification of Diabetes: Standards of Care in Diabetes-2024. Diabetes Care *47* (*Supplement 1*), S20–S42. https://doi.org/10.2337/dc24-S002.
39. Trenti, T., Cristani, A., Cioni, G., Pentore, R., Mussini, C., and Ventura, E. (1990). Fructosamine and glycated hemoglobin as indices of glycemic control in patients with liver cirrhosis. Ric. Clin. Lab. *20*, 261–267. https://doi.org/10.1007/BF02900711.
40. Nomura, Y., Nanjo, K., Miyano, M., Kikuoka, H., Kuriyama, S., Maeda, M., and Miyamura, K. (1989). Hemoglobin A1 in cirrhosis of the liver. Diabetes Res. *11*, 177–180. https://www.ncbi.nlm.nih.gov/pubmed/2625033.
41. Cacciatore, L., Cozzolino, G., Giardina, M.G., De Marco, F., Sacca, L., Esposito, P., Francica, G., Lonardo, A., Matarazzo, M., and Varriale, A. (1988). Abnormalities of glucose metabolism induced by liver cirrhosis and glycosylated hemoglobin levels in chronic liver disease. Diabetes Res. *7*, 185–188. https://www.ncbi.nlm.nih.gov/pubmed/3402168.
42. Forbes, S., Oram, R.A., Smith, A., Lam, A., Olateju, T., Imes, S., Malcolm, A.J., Shapiro, A.M., and Senior, P.A. (2016). Validation of the BETA-2 Score: An Improved Tool to Estimate Beta Cell Function After Clinical Islet Transplantation Using a Single Fasting Blood Sample. Am. J. Transplant *16*, 2704–2713. https://doi.org/10.1111/ajt.13807.
43. Bachul, P.J., Gołębiewska, J.E., Basto, L., Gołąb, K., Anteby, R., Wang, L.J., Tibudan, M., Thomas, C., Fendler, W., Lucander, A., et al. (2020). BETA-2 score is an early predictor of graft decline and loss of insulin independence after pancreatic islet allotransplantation. Am. J. Transplant *20*, 844–851. https://doi.org/10.1111/ajt.15645.
44. Marfil-Garza, B.A., Imes, S., Verhoeff, K., Hefler, J., Lam, A., Dajani, K., Anderson, B., O'Gorman, D., Kin, T., Bigam, D., et al. (2022). Pancreatic islet transplantation in type 1 diabetes: 20-year experience from a single-centre cohort in Canada. Lancet Diabetes Endocrinol. *10*, 519–532. https://doi.org/10.1016/S2213-8587(22)00114-0.
45. Lam, A., Oram, R.A., Forbes, S., Olateju, T., Malcolm, A.J., Imes, S., Shapiro, A.M.J., and Senior, P.A. (2022). Estimation of Early Graft Function Using the BETA-2 Score Following Clinical Islet Transplantation. Transpl. Int. *35*, 10335. https://doi.org/10.3389/ti.2022.10335.
46. Akçay, A., Dönmez, Z., Peker, A.A., Toprak, H., and Gültekin, M.A. (2024). Diagnostic utility of Magnetic Resonance Imaging in discriminating immature teratoma: Insights from a case series. J. Clin. Ultrasound. https://doi.org/10.1002/jcu.23715.
47. Talerman, A., Haije, W.G., and Baggerman, L. (1980). Serum alphafetoprotein (AFP) in patients with germ cell tumors of the gonads and extragonadal sites: correlation between endodermal sinus (yolk sac) tumor and raised serum AFP. Cancer *46*, 380–385. https://doi.org/10.1002/1097-0142(19800715)46:2<380::aid-cncr2820460228>3.0.co;2-u.
48. Irie, T., Watanabe, H., Kawaoi, A., and Takeuchi, J. (1982). alpha-Fetoprotein (AFP), human chorionic gonadotropin (HCG), and carcinoembryonic antigen (CEA) demonstrated in the immature glands of mediastinal teratocarcinoma: a case report. Cancer *50*, 1160–1165. https://doi.org/10.1002/1097-0142(19820915)50:6<1160::aid-cncr2820500621>3.0.co;2-5.
49. Szymendera, J.J., Zborzil, J., Sikorowa, L., Leńko, J., Kamińska, J.A., and Gadek, A. (1983). Evaluation of five tumor markers (AFP, CEA, hCG, hPL and SP1) in monitoring therapy and follow-up of patients with testicular germ cell tumors. Oncology *40*, 1–10. https://doi.org/10.1159/000225681.
50. El Malahi, A., Van Elsen, M., Charleer, S., Dirinck, E., Ledeganck, K., Keymeulen, B., Crenier, L., Radermecker, R., Taes, Y., Vercammen, C., et al. (2022). Relationship Between Time in Range, Glycemic Variability, HbA1c, and Complications in Adults With Type 1 Diabetes Mellitus. J. Clin. Endocrinol. Metab. *107*, e570–e581. https://doi.org/10.1210/clinem/dgab688.
51. Beck, R.W., Bergenstal, R.M., Riddlesworth, T.D., Kollman, C., Li, Z., Brown, A.S., and Close, K.L. (2019). Validation of Time in Range as an Outcome Measure for Diabetes Clinical Trials. Diabetes Care *42*, 400–405. https://doi.org/10.2337/dc18-1444.
52. Stratton, I.M., Adler, A.I., Neil, H.A., Matthews, D.R., Manley, S.E., Cull, C.A., Hadden, D., Turner, R.C., and Holman, R.R. (2000). Association of glycaemia with macrovascular and microvascular complications of type 2 diabetes (UKPDS 35): prospective observational study. BMJ *321*, 405–412. https://doi.org/10.1136/bmj.321.7258.405.
53. Wood, J.R., Miller, K.M., Maahs, D.M., Beck, R.W., DiMeglio, L.A., Libman, I.M., Quinn, M., Tamborlane, W.V., and Woerner, S.E.; T1D Exchange Clinic Network (2013). Most youth with type 1 diabetes in the T1D Exchange Clinic Registry do not meet American Diabetes Association or International Society for Pediatric and Adolescent Diabetes clinical guidelines. Diabetes Care *36*, 2035–2037. https://doi.org/10.2337/dc12-1959.
54. Miller, K.M., Foster, N.C., Beck, R.W., Bergenstal, R.M., DuBose, S.N., DiMeglio, L.A., Maahs, D.M., and Tamborlane, W.V.; T1D Exchange Clinic Network (2015). Current state of type 1 diabetes treatment in the U.S.: updated data from the T1D Exchange clinic registry. Diabetes Care *38*, 971–978. https://doi.org/10.2337/dc15-0078.
55. Foster, N.C., Beck, R.W., Miller, K.M., Clements, M.A., Rickels, M.R., DiMeglio, L.A., Maahs, D.M., Tamborlane, W.V., Bergenstal, R., Smith, E., et al. (2019). State of Type 1 Diabetes Management and Outcomes from the T1D Exchange in 2016-2018. Diabetes Technol. Ther. *21*, 66–72. https://doi.org/10.1089/dia.2018.0384.
56. Hankosky, E.R., Schapiro, D., Gunn, K.B., Lubelczyk, E.B., Mitroi, J., and Nelson, D.R. (2023). Gaps Remain for Achieving HbA1c Targets for People with Type 1 or Type 2 Diabetes Using Insulin: Results from NHANES 2009-2020. Diabetes Ther. *14*, 967–975. https://doi.org/10.1007/s13300-023-01399-0.
57. Foster, E.D., Bridges, N.D., Feurer, I.D., Eggerman, T.L., Hunsicker, L.G., and Alejandro, R.; Clinical; Islet; Transplantation Consortium (E.D.) (2018). Improved Health-Related Quality of Life in a Phase 3 Islet Transplantation Trial in Type 1 Diabetes Complicated by Severe Hypoglycemia. Diabetes Care *41*, 1001–1008. https://doi.org/10.2337/dc17-1779.
58. Rickels, M.R. (2019). Hypoglycemia-associated autonomic failure, counterregulatory responses, and therapeutic options in type 1 diabetes. Ann. N. Y. Acad. Sci. *1454*, 68–79. https://doi.org/10.1111/nyas.14214.
59. Brusko, T.M., Russ, H.A., and Stabler, C.L. (2021). Strategies for durable beta cell replacement in type 1 diabetes. Science *373*, 516–522. https://doi.org/10.1126/science.abh1657.
60. Reichman, T.W., Ricordi, C., Naji, A., Markmann, J.F., Perkins, B.A., Wijkstrom, M., Paraskevas, S., Bruinsma, B., Marigowda, G., and Shih, J.L. (2023). 836-P: Glucose-Dependent Insulin Production and Insulin-Independence in Type 1 Diabetes from Stem Cell–Derived, Fully Differentiated Islet Cells—Updated Data from the VX-880 Clinical Trial. Diabetes *72*. https://doi.org/10.2337/db23-836-P.
61. Hou, P., Li, Y., Zhang, X., Liu, C., Guan, J., Li, H., Zhao, T., Ye, J., Yang, W., Liu, K., et al. (2013). Pluripotent stem cells induced from mouse somatic cells by small-molecule compounds. Science *341*, 651–654. https://doi.org/10.1126/science.1239278.

62. Zhang, M., Wang, L., An, K., Cai, J., Li, G., Yang, C., Liu, H., Du, F., Han, X., Zhang, Z., et al. (2018). Lower genomic stability of induced pluripotent stem cells reflects increased non-homologous end joining. Cancer Commun. (Lond) *38*, 49. https://doi.org/10.1186/s40880-018-0313-0.

63. Ping, W., Hu, J., Hu, G., Song, Y., Xia, Q., Yao, M., Gong, S., Jiang, C., and Yao, H. (2018). Genome-wide DNA methylation analysis reveals that mouse chemical iPSCs have closer epigenetic features to mESCs than OSKM-integrated iPSCs. Cell Death Dis. *9*, 187. https://doi.org/10.1038/s41419-017-0234-x.

64. Tian, C., Liu, L., Ye, X., Fu, H., Sheng, X., Wang, L., Wang, H., Heng, D., and Liu, L. (2019). Functional Oocytes Derived from Granulosa Cells. Cell Rep. *29*, 4256–4267.e9. https://doi.org/10.1016/j.celrep.2019.11.080.

65. Hao, Y., Stuart, T., Kowalski, M.H., Choudhary, S., Hoffman, P., Hartman, A., Srivastava, A., Molla, G., Madad, S., Fernandez-Granda, C., and Satija, R. (2024). Dictionary learning for integrative, multimodal and scalable single-cell analysis. Nat. Biotechnol. *42*, 293–304. https://doi.org/10.1038/s41587-023-01767-y.

66. Li, H., and Durbin, R. (2009). Fast and accurate short read alignment with Burrows-Wheeler transform. Bioinformatics *25*, 1754–1760. https://doi.org/10.1093/bioinformatics/btp324.

67. Wang, K., Li, M., and Hakonarson, H. (2010). ANNOVAR: functional annotation of genetic variants from high-throughput sequencing data. Nucleic Acids Res. *38*, e164. https://doi.org/10.1093/nar/gkq603.

68. Stuart, T., Butler, A., Hoffman, P., Hafemeister, C., Papalexi, E., Mauck, W.M., 3rd, Hao, Y., Stoeckius, M., Smibert, P., and Satija, R. (2019). Comprehensive Integration of Single-Cell Data. Cell *177*, 1888–1902.e21. https://doi.org/10.1016/j.cell.2019.05.031.

69. Forbes, S. (2021). The BETA-2 score web app calculator: https://www.beta2score.com/ for assessment of graft function following islet transplantation. Am. J. Transplant *21*, 2619. https://doi.org/10.1111/ajt.16551.

STAR★METHODS

KEY RESOURCES TABLE

REAGENT or RESOURCE	SOURCE	IDENTIFIER
Antibodies		
Mouse anti-NKX6.1 antibody	DSHB	Cat# F55A12; RRID: AB_532379
Rat anti-C-peptide antibody	DSHB	Cat# GN-ID4; RRID: AB_2255626
Mouse anti-Somatostatin antibody	Santa Cruz	Cat# sc-55565; RRID: AB_831726
Mouse anti-Glucagon antibody	Santa Cruz	Cat# sc-514592; RRID: AB_2629431
Rabbit anti-Glucagon antibody	Servicebio	Cat# GB13097
Mouse anti-NKX6.1 antibody	DSHB	Cat# F55A12; RRID: AB_532379
Goat anti-PDX1 antibody	R&D system	Cat# AF2419; RRID: AB_355257
Mouse monoclonal anti-OCT4	BD Biosciences	Cat# 611203; RRID: AB_398737
Rabbit monoclonal anti-OCT4	Invitrogen	Cat# MA5-14845; RRID: AB_10979606
Goat polyclonal anti-SOX2	R&D	Cat# AF2018; RRID: AB_355110
Rabbit polyclonal anti-NANOG	Abcam	Cat# ab21624; RRID: AB_446437
Mouse monoclonal anti-TRA-1-60	Millipore	Cat# MAB4360; RRID: AB_2119183
Mouse monoclonal anti-TRA-1-81	Millipore	Cat# MAB4381; RRID: AB_177638
Mouse polyclonal anti-SSEA-4	Santa Cruz	Cat# sc-21704; RRID: AB_628289
Rabbit anti-Insulin antibody (Rabbit)	Abcam	Cat# ab63820; RRID:AB_1925116
Rabbit anti-CHGA antibody	Abcam	Cat# AB68271; RRID: AB_11154750
Sheep anti-TPH1 antibody	Sigma-Aldrich	Cat# AB1541; RRID: AB_90754
Alexa Fluor 488-AffiniPure Donkey Anti-Mouse IgG (H+L)	Jackson Immuno Research	Cat# 715-545-150; RRID: AB_2340846
Alexa Fluor 488-AffiniPure Donkey Anti-Rabbit IgG (H+L)	Jackson Immuno Research	Cat# 711-545-152; RRID: AB_2313584
Alexa Fluor 488-AffiniPure Donkey Anti-Goat IgG (H+L)	Jackson Immuno Research	Cat# 705-545-147; RRID: AB_2336933
Cy3-AffiniPure Donkey Anti-Rabbit IgG (H+L)	Jackson Immuno Research	Cat# 711-165-152; RRID: AB_2307443
Cy3-AffiniPure Donkey Anti-Mouse IgG (H+L)	Jackson Immuno Research	Cat# 715-165-150; RRID: AB_2340813
Cy3-AffiniPure Donkey Anti-Goat IgG (H+L)	Jackson Immuno Research	Cat# 705-165-147; RRID: AB_2307351
Alexa Fluor 647 Donkey Anti-Goat IgG (H+L)	Jackson Immuno Research	Cat# 705-605-147; RRID: AB_2340437
Alexa Fluor 647 Donkey Anti-Mouse IgG (H+L)	Jackson Immuno Research	Cat# 715-605-150; RRID: AB_2340862
Alexa Fluor 647 Donkey Anti-Rabbit IgG (H+L)	Jackson Immuno Research	Cat# 711-605-152; RRID: AB_2492288
Chemicals, peptides, and recombinant proteins		
NaCl	RHAWN, China	Cat# 19773500
KCl	HUSHI, China	Cat# 10016318
NaHCO3	HUSHI, China	Cat# 10018960
MgSO4-7H2O	HUSHI, China	Cat# 10013018
KH2PO4	HUSHI, China	Cat# 10017618
CaCl2-2H2O	Sigma-Aldrich	Cat# 10043-52-4
$ZnSO_4$	Sigma-Aldrich	Cat# Z0251
Valproic acid sodium salt (VPA)	Sigma-Aldrich	Cat# P4543
CHIR99021	WUXI APPTEC	N/A
616452	WUXI APPTEC	N/A
Tranylcypromine	Enzo	Cat# BML-EI217-0005
3-deazaneplanocin A (DZNep)	WUXI APPTEC	N/A
PD0325901	WUXI APPTEC	N/A
EPZ5676	MCE	Cat# HY-15593
TTNPB	WUXI APPTEC	N/A
Y-27632	WUXI APPTEC	N/A
SAG	WUXI APPTEC	N/A

(*Continued on next page*)

Continued

REAGENT or RESOURCE	SOURCE	IDENTIFIER
Recombinant Human FGF2	Origene	Cat# TP750002
5-Azacytidine	Sigma-Aldrich	Cat# A2385
JNKIN8	Selleckchem	Cat# S4901
Recombinant Human Heregulinb-1 (HRG)	PEPROTECH	Cat# 100-03
SB590885	Selleckchem	Cat# S2220
Ruxolitinib	Selleckchem	Cat# S1378
DMH-1	Selleckchem	Cat# S7146
dB-cAMP	Selleckchem	Cat# S7858
BMP4	Stemimmune LLC	Cat# HST-B4-0100
ABT-869	WUXI APPTEC	N/A
UNC0224	MCE	Cat# HY-10929
IWP-2	Selleckchem	Cat# S7085
LIF	PeproTech	Cat# 300-05
ACTIVIN A	StemimmuneLLC	Cat# HST-A-0100
KGF	Stemimmune LLC	Cat# HST-F7-1000
EGF	Peprotech	Cat# AF-100-15
PI103	Selleck	Cat# S1038
Vitamin C (Vc)	Sigma-Aldrich	Cat# 49752
SB431542	Selleck	Cat# S1067
Wnt-C59	Selleck	Cat# S7037
LDN193189	Selleck	Cat# S7507
Retinoic acid (RA)	Sigma-Aldrich	Cat# R2625
Sant1	Selleck	Cat# S7092
Nicotinamide (NAM)	Sigma-Aldrich	Cat# N0636
TPB	Adooq Bioscience	Cat# A13094
ALK5 inhibitor II	Selleck	Cat# S7223
Liothyronine Sodium (T3)	Selleck	Cat# S4217
Isoxazole 9 (ISX9)	Selleck	Cat# S7914
γ-Secretase Inhibitor XX (Xxi)	Calbiochem	Cat# 565789
R428	Selleck	Cat# S2841
N-Acetyl-L-cysteine (Nac)	Sigma-Aldrich	Cat# A9165
Glucose	Sigma-Aldrich	Cat# G7021
Critical commercial assays		
Human Insulin ELISA kit	Mercodia, Sweden	Cat# 10-1131-01
Human C-peptide ELISA kit	ALPCO	Cat# 80-CPTHU-E10
Human Glucagon ELISA kit	Mercodia	Cat# 10-1271-01
BCA protein assay kit	Solarbio, Beijing	Cat# PC0020
Deposited data		
Single-cell RNA-seq data of recovered CiPSC-islets (before transplantation)	This paper	GSA for Human: HRA006309
WGS/WES data generated for the patient's ADSCs, CiPSC-#8 line and the patient's CiPSC-islets	This paper	GSA for Human: HRA007623
Oligonucleotides		
GAPDH: Forward: TGACATCAAGAAGGTGGTGAAGCAGG Reverse: GCGTCAAAGGTGGAGGAGTGGGT	Beijing Tsingke Biotech Co., Ltd.	N/A
POU5F1: Forward: CTGGGTTGATCCTCGGACCT Reverse: CCATCGGAGTTGCTCTCCA	Beijing Tsingke Biotech Co., Ltd.	N/A

(*Continued on next page*)

Continued

REAGENT or RESOURCE	SOURCE	IDENTIFIER
SOX2: Forward: TTGCGTGAGTGTGGATGGGATTGGTG Reverse: GGGAAATGGGAGGGGTGCAAAAGAGG	Beijing Tsingke Biotech Co., Ltd.	N/A
NANOG: Forward: GATTTGTGGGCCTGAAGAAA Reverse: CAGATCCATGGAGGAAGGAA	Beijing Tsingke Biotech Co., Ltd.	N/A
LIN28: Forward: TTTCCCTCATTCCTGAACTGC Reverse: CAGCAAAATCAACCATCAAATAAAC	Beijing Tsingke Biotech Co., Ltd.	N/A
SALL4: Forward: AGCACATCAACTCGGAGGAG Reverse: CATTCCCTGGGTGGTTCACTG	Beijing Tsingke Biotech Co., Ltd.	N/A
DPPA4: Forward: GCTAACATCTGCCACCCCACCA Reverse: GGATTCTGCGGTGCTGCTGACA	Beijing Tsingke Biotech Co., Ltd.	N/A
UTF1: Forward: CGCCGCTACAAGTTCCTTAAA Reverse: GGATCTGCTCGTCGAAGGG	Beijing Tsingke Biotech Co., Ltd.	N/A
PRDM14: Forward: TTGAGGAAGAGAATCAGATCCAG Reverse: CGTTCTGTACGGGGTCACTC	Beijing Tsingke Biotech Co., Ltd.	N/A
ZIC3: Forward: CAGGAGCTGTCGTGCAAGT Reverse: AGTAGCAGACGTGGTTGTTCT	Beijing Tsingke Biotech Co., Ltd.	N/A
ZFP42: Forward: AGAAACGGGCAAAGACAAGAC Reverse: GCTGACAGGTTCTATTTCCGC	Beijing Tsingke Biotech Co., Ltd.	N/A
TERT: Forward: GCCGATTGTGAACATGGACTACG Reverse: GCTCGTAGTTGAGCACGCTGAA	Beijing Tsingke Biotech Co., Ltd.	N/A
CDH1: Forward: GCCTCCTGAAAAGAGAGTGGAAG Reverse: TGGCAGTGTCTCTCCAAATCCG	Beijing Tsingke Biotech Co., Ltd.	N/A
EPCAM: Forward: GCCAGTGTACTTCAGTTGGTGC Reverse: CCCTTCAGGTTTTGCTCTTCTCC	Beijing Tsingke Biotech Co., Ltd.	N/A
Software and algorithms		
Prism (ver. 9.5)	GraphPad	https://www.graphpad.com
BD Accuri C6 Plus Analysis Software	BD BioSciences	https://www.bdbiosciences.com
Flow Jo vX	Flow Jo	https://www.flowjo.com
Base R (ver. 4.3.2)	R Development Core Team	https://www.r-project.org
Cell Ranger (ver. 7.2.0)	10x Genomics	https://support.10xgenomics.com
Seurat (ver. 5.0.0)	Hao et al., 2024[65]	https://satijalab.org/seurat
BWA-MEM (ver. 0.7.10)	Li, et al.[66]	https://bio-bwa.sourceforge.net
GATK (ver. 4.2.5.0)	Broad Institute	https://gatk.broadinstitute.org/hc/en-us
Control-FREEC (ver. 11.6)	BOEVA Lab	https://boevalab.inf.ethz.ch/FREEC
ANNOVAR (ver. 2020Jun08)	Wang, et al.[67]	https://annovar.openbioinformatics.org
COSMIC (ver. 97)	Sanger Institute	https://cancer.sanger.ac.uk/cosmic
BETA-2 scores	https://www.beta2score.com	https://www.beta2score.com
Other		
Mesenchymal Stem Cell Growth Medium 2	PromoCell	Cat# C-28009
Mesenchymal Stem Cell Growth Medium supplement mix	PromoCell	Cat# C-39809

(*Continued on next page*)

Continued

REAGENT or RESOURCE	SOURCE	IDENTIFIER
Accutase	EMD Millipore	Cat# SCR005
Matrigel	BD BioSciences	Cat# 356231
mTeSR1 medium	STEMCELL	Cat# 85850
mTeSR™ Plus Medium	STEMCELL	Cat# 100-0276
DMEM-basic medium	Gibco	Cat# 11054020
DMEM	Gibco	Cat# 11965500BT
KnockOut™ DMEM	Gibco	Cat# 10829018
N2 supplement	Gibco	Cat# 17502-048
B27 supplement	Gibco	Cat# 17504-044
MCDB131	Gibco	Cat# 10372-019
Fetal Bovine Serum (FBS)	Vistech	Cat# VIS93526487
Knockout Serum Replacement (KSR)	Gibco	Cat# 10828028
Penicillin-Streptomycin	Gibco	Cat# 15140-122
Collagenase IV	Gibco	Cat# 1963347
GlutaMAX™	Gibco	Cat# 35050-061
Trypsin-EDTA	Gibco	Cat# 25200-056
MEM Non-Essential Amino Acids Solution (NEAA)	Gibco	Cat# 11140050
CMRL1066	Corning	Cat# 15-110-CV
Matrigel	Corning	Cat# 354248
Human serum albumin	CSL Behring	Cat# 113615
Trypsin-EDTA	Gibco	Cat# 25200-056
Trypan blue	Invitrogen	Cat# T10282
Dithizone (DTZ)	Sigma-Aldrich	Cat# D5130
Fluorescein diacetate (FDA)	Sigma-Aldrich	Cat# F7378
Propidium iodide (PI)	Sigma-Aldrich	Cat# P4170
Fixation/Permeabilization Solution	BD BioSciences	Cat# 554714
Perm/Wash™ Buffer	BD BioSciences	Cat# 554723
AlbuMAX™-II	Gibco	Cat# 11021-045
ReLeSR™	STEMCELL	Cat# 05872
PBS	Corning	Cat# 05418005
BSA	Sigma-Aldrich	Cat# A4612
Heparin sodium	Selleck	Cat# S1346
RIPA buffer	Thermo Fisher Scientific	Cat# 89900
DMSO	Sigma-Aldrich	Cat# D2650

EXPERIMENTAL MODEL AND STUDY PARTICIPANT DETAILS

The study was conducted in accordance with the Declaration of Helsinki and was approved by the National Health Commission of the People's Republic of China and the Medical Ethics Committee at Tianjin First Central Hospital, and was conducted in accordance to the Clinical Study Protocol (Data S1). Prior to the start of patient recruitment, the trial was registered in the Chinese Clinical Trial Registry (registration number: ChiCTR2300072200). In this report, we present data from the clinical trial's first participant—a 25-year-old female with an 11-year history of T1D. Before CiPSC-islets transplantation, the patient had undergone two liver transplants on July 8th, 2014 and September 27th, 2016, for liver cryptogenic cirrhosis. In addition, a whole pancreas transplantation was performed on May 4th, 2017, but the pancreas graft was removed one year later (August 8th, 2018) due to thrombotic complications. The current patient provided written informed consent to undergo the procedure.

METHOD DETAILS

Generation of CiPSCs from the patient's adipose-derived mesenchymal stromal cells

The procedure for generation of patient CiPSCs and in-process and release quality control was detailed in Method S1. Briefly, adipose tissue near 30 mL in volume was obtained from abdominal subcutaneous fat of the patient and cultured to obtain adipose-derived

mesenchymal stromal cells (ADSCs). The tissues were washed twice with PBS containing 2% penicillin–streptomycin, dissociated with 5–10 mL collagenase IV solution (final concentration 2 mg/mL) in a 100 mm dish at 37 °C for 30 min. Next, 10–20 mL of 15% FBS-DMEM medium was added, and the cells were pipetted up and down several times for dissociation. The suspension was collected to two 50 mL tubes and diluted to 30–40 mL each with 15% FBS-DMEM medium, followed by shaking for 1–2 min to release cells. The suspension was then centrifuged at 400 x g for 5 min. After the supernatant was removed, the cells were resuspended in mesenchymal stem cell growth medium 2 (PromoCell, C-28009) with supplement mix (PromoCell, C-39809). Dissociated cells obtained and were plated in 2 wells of 6-well plates (P0) followed by incubation at 37 °C under 5% CO_2. The next day, fresh mesenchymal stem cell growth medium 2 was changed to remove the non-adherent cells. Primary ADSCs become confluent in 7 days and were ready to be passaged for re-programming. Medium was changed every 3-4 d. Primary ADSCs were passaged using Accutase (Millipore) when confluent, usually every 3-5 d. Autologous feeder cells were prepared by exposing an expanded culture of the patient's ADSCs to mitomycin C (10 μg/mL) for 3 h, and then plating the treated feeder cells the day before use.

For the CiPSC induction, a four step chemical reprogramming protocol without genetic manipulation was applied to patient ADSCs as described previously.[4] ADSCs were seeded at a density of 1 × 10^4 cells per well of a 12-well plate in 15% FBS-DMEM medium. The medium was changed into stage 1 induction medium the next day. The formula of the stage-specific culture medium is provided in the table below.

Stage	Day	Medium components	Factors added	Concentration of factors
Stage 1	Days 1–14	KnockOut DMEM	CHIR999021	10 μM
		KSR 10%	616452	10 μM
		FBS 10%	TTNPB	2 μM
		GlutaMax 1%	SAG	0.5 μM
		NEAA 1%	ABT-869	1 μM
		2-mercaptoethanol 0.055 mM	Y-27632	2 μM
		penicillin–streptomycin 1%	EPZ5676	2 μM
		Vc 50 μg/ml	DZNep	0.02 μM
		LiCl 5mM	Ruxolitinib	1 μM
		NAM 1 mM	dB-cAMP	10 μM
		AlbuMax-II 2 mg/ml	BMP4	20 ng/ml (first 6 days)
Stage 2	Days 15–40	KnockOut DMEM	CHIR99021	12 μM
		KSR 10%	616452	10 μM
		FBS 10%	TTNPB	2 μM
		GlutaMax 1%	SAG	0.5 μM
		NEAA 1%	ABT-869	1 μM
		2-mercaptoethanol 0.055 mM	Y-27632	10 μM
		penicillin–streptomycin 1%	JNKIN8	1 μM
		Vc 50 μg/ml	tranylcypromine	2 μM
		LiCl 5mM	5-azacytidine	10 μM
		NAM 1 mM	UNC0224	1 μM
		bFGF 100 ng/ml	DMH-1	0.5uM
			dB-cAMP	10 μM
Stage 3	Days 41–48	KnockOut DMEM	CHIR99021	1 μM
		N2 supplement 1%	616452	10 μM
		B27 supplement 2%	Y-27632	10 μM
		GlutaMax 1%	PD0325901	1 μM
		NEAA 1%	tranylcypromine	10 μM
		2-mercaptoethanol 0.055 mM	VPA	500 μM
		penicillin–streptomycin 1%	DZNep	0.2 μM
		Vc 50 μg/ml	EPZ004777	5 μM
		AlbuMax-II 5 mg/ml	JNKIN8	1 μM
		HRG 20 ng/ml		

(*Continued on next page*)

Continued

Stage	Day	Medium components	Factors added	Concentration of factors
Stage 4	Days 49–59	KnockOut DMEM	CHIR99021	1 μM
		N2 supplement 1%	Y-27632	10 μM
		B27 supplement 2%	PD0325901	1 μM
		GlutaMax 1%	IWP-2	2 μM
		NEAA 1%	SB590885	0.5 μM (first 4 days)
		2-mercaptoethanol 0.055 mM	VPA	500 μM (first 4 days)
		penicillin–streptomycin 1%	LIF	10 ng/mL
		Vc 50 μg/ml	ACTIVIN A	5 ng/mL
		HRG 20 ng/ml		

After the four-stage process, cells were dissociated by Accutase (Millipore) and replated at a ratio of 1:6 on autologous feeder layers in the modified stage IV condition: KnockOut DMEM supplemented with 1% N2 supplement, 2% B27 supplement, 1% GlutaMax, 1% NEAA, 1% penicillin–streptomycin, 0.055 mM 2-mercaptoethanol, 50 μg/mL Vc2p and the small molecules CHIR99021 (1 μM), PD0325901 (0.1 μM), Y-27632 (10 μM), HRG (20 ng/mL), LIF (10 ng/mL), ACTIVIN A (5ng/mL) and bFGF (40 ng/mL, Origene). After 12 days, compact CiPS cell colonies appeared. In total, 23 colonies of CiPSC were manually picked up and mechanically dissociated into small clumps and transferred onto Matrigel-coated (BD BioSciences, 356231) plates in mTeSR1 medium (STEMCELL) supplemented with Y-27632 (10 μM) for the first day before replacing the medium with fresh mTeSR1 medium without Y-27632. Subsequently, the patient CiPSC clones were subject to the following evaluations to select a cell line for downstream manufacture. Karyotype screen of the 23 clones with good morphology and normal cell growth showed abnormal karyotype in one, #11, which was removed from downstream screening. The remaining 22 clones were then subject to our islet differentiation protocol. All patient CiPSC clones tested showed the ability to differentiate into beta cells, and the one with the highest cell yield was chosen for downstream manufacture (patient CiPSC-#8). Short tandem repeat (STR), whole genome sequencing (WGS) and whole exome sequencing (WES) tests were conducted on the selected clone #8, which passed all the tests.

Patient CiPSCs lines were maintained in mTeSR1 medium on Matrigel-coated plates under 21% O_2 and 5% CO_2 at 37 °C. The medium was changed every day. Cells were passaged when they reached around 85% confluence. This typically occurred at day 5–7 after passaging with split ratios of around 1:10 to 1:12. For passaging, CiPS cells were dissociated by ReLeSR (StemCell), and the detached cell aggregates were transferred onto Matrigel-coated plates in mTeSR1 medium supplemented with Y-27632 (10 μM). The colonies were allowed to attach to the culture plate for 24 h before replacing the medium with fresh mTeSR1 medium without Y-27632.

Cryopreservation of patient CiPSC was perfomed after expansion. In brief, patient CiPSC were dissociated by ReLeSR, and the detached cell aggregates were suspended in cryopreservation medium (10% dimethylsulfoxide (Sigma-Aldrich, D2650), 90% FBS and 10 μM Y27632). Then, the suspension was aliquoted into 2 mL vials as a 1 mL cell suspension each. All cell preparations were conducted at a GMP-level cell processing facility (Hangzhou Reprogenix Bioscience).

Assessment of patient CiPSC clones

The patient CiPSC-#8 cell line was assessed for quality according to the requirements in Table S1 Part 1. Cell viability was evaluated by trypan blue staining in approximately 1 million or more dissociated cells. The expression of stem cell markers was confirmed by immunocytochemistry using anti-SSEA-4 (Cat# sc-21704: Santa Cruz), anti-TRA-60 (Cat# MAB4360: Millipore), anti-TRA-1-81 (Cat# MAB4381: Millipore), anti-Oct-3/4 (Cat# 611203: BD Biosciences), goat polyclonal anti-SOX2 (Cat# AF2018: R&D) and rabbit polyclonal anti-NANOG (Cat# ab21624: Abcam) antibodies as previously described.[4]

For karyotype analysis, karyotype integrity was analyzed in 1000 different metaphase cells by G-band after Giemsa staining for each clone, following criteria specified by the Chinese Pharmacopoeia (ISBN: 9780118987677), which is a compendium of national guidelines that describes statutory technical specifications that must be adhered to in drug development, production and use. The genetic stability of the patient CiPSC-#8 clone was further analyzed in detail by whole genome/exome sequencing (WGS/WES), described in later sections.

The *in vitro* infectious pathogen test was performed at Wuhan Canvest Biotechnology (CMA- and CNAS-certified qualified GLP facility) using a 14/28-day *in vitro* assay and evaluated cytopathic effects on 2BS and Vero cells, followed by haemadsorption and hemagglutination test. The *in vivo* infectious pathogen test was performed by inoculation into animals for 21-42 days and chicken embryos for 3-5 days, subsequently evaluating survival rate and hemagglutination test to determine infections caused by transmissible factors or viruses (report number: 012103812).

The reagents used in the entire manufacturing process was subject to reagent controls, including checking documentation of certificates of analysis (COA) of every reagent. For reagents containing components of animal-origin, additional tests were conducted to control for the associated risks including detection of murine viruses by real-time quantitative PCR, detection of bovine viruses by haemadsorption and fluorescence antibody test.

Preparation of CiPSC-islets and safety assessment

The procedure for the preparation of CiPSC-islets is summarized in Methods S1.

The differentiation of CiPSCs into islets and cryopreservation and recovery of CiPSC-islets were described previously.[20] Briefly, patient CiPSC-#8 were dispersed into single cells with Accutase (EMD Millipore, SCR005) and seeded at an approximate density of 3 × 10^8 cells per 5-layer cell factory (Nest Biotech, 771204), which were coated using Matrigel. Differentiation was initiated 24 h after seeding. The compositions of the differentiation stage-specific culture media are provided in the table below.

Stage	Day	Medium Ingredients	Factors	Concentration
Stage 1	Day 1	MCDB131	Activin A	100 ng/mL
		Glucose 4.5 mM	Vitamin C	0.25 mM
		GlutaMAX 1%	Chir99021	6 μM
		B27 1%	PI103	50 nM
		Pen/Strep 1%	Y27632	10 μM
	Days 2–4		Activin A	50 ng/mL
			Vitamin C	0.25 mM
Stage 2	Days 5–6	MCDB131	KGF	50 ng/mL
		Glucose 4.5 mM	Vitamin C	0.25 mM
		GlutaMAX 1%	SB431542	5 μM
		B27 1%	Wnt-C59	100 nM
		Pen/Strep 1%		
Stage 3	Days 7–10	DMEM-Basic	Retinoic acid	2 μM
		B27 1%	LDN193189	0.1 μM
		Pen/Strep 1%	Sant1	0.25 μM
			Wnt-C59	100 nM
Stage 4	Days 11–16	DMEM-Basic	EGF	100 ng/mL
		GlutaMAX 1%	TPB	0.2 μM
		B27 1%	Nicotinamide	10 mM
		Pen/Strep 1%	Sant1	0.25 μM
			Vitamin C	0.25 mM
Stage 5	Days 17–22	MCDB131	ALK5 inhibitor II	10 μM
		GlutaMAX 1%	LDN193189	0.3 μM
		B27 1%	T3	1 μM
		Pen/Strep 1%	ISX9	10 μM (first 3 days)
			Heparin	10 μg/mL
			Xxi	0.1 μM
			Wnt-C59	100 nM
			Y27632	10 μM
			Vitamin C	0.25 mM
Stage 6	Days 23–25	MCDB131	ALK5 inhibitor II	10 μM
		B27 1%	R428	0.5 μM
		Pen/Strep 1%	T3	1 μM
			Vitamin C	0.25 mM
			Heparin	10 μg/mL
			Zinc sulfate	10 μM
			Nac	2 mM

The adherent cells were transferred into 3D culture at the end of stage 3. After dispersing with Accutase, single cells were seeded in six-well AggreWell™ 400 Microwell Plates (STEMCELL Technologies, 27940) at a density of 1.16 × 10^7 per well (not per microwell) in stage 4 differentiation medium supplemented with 10 μM Y27632 (Selleckchem, S1049). Uniform cell clusters were formed after 24 h, which were collected and transferred into ultra-low attachment six-well plates (Beaver Bio, 40406). Cell aggregates were further differentiated according to the differentiation protocol, with Stage 4 to final Stage 6 culture occurring in an incubator shaker (INFORS HT, Multitron) operating at a rotation rate of 90 r.p.m. at 37 °C, 5% CO_2 concentration and 85% humidity.

Cryopreservation of patient CiPSC-#8-derived islets (hereafter referred to as patient CiPSC-islets) was perfomed after differentiation. In brief, patient CiPSC-derived islets were dissociated into single cells using Accutase and after counting with Countess II Automated Cell Counter (Invitrogen, AMQAX1000), cells were suspended at 3×10^7 cells/mL in cryopreservation medium (5% dimethylsulfoxide (DMSO) (Sigma-Aldrich, D2650), 60% stage 6 medium, 35% FBS and 10 μM Y27632). Then, a 4 mL cell suspension was aliquoted into 5 mL vials. Cryopreservation was conducted in a Thermo Scientific CryoMed (Thermo Fisher). The vials were stored long term or transported in liquid nitrogen (the transportation process is detailed in a later section).

The differentiating and Stage 6 patient CiPSC-islets used for clinical transplantation were assessed to meet quality standards according to the list of requirement standards in Table S1 Part 2. Purity and potency was quantified by pancreatic endocrine marker CHGA positive cells and percentage of NKX6.1$^+$C-peptide$^+$ cells of dissociated Stage 6 CiPSC-islets. The secretion of C-peptide and Glucagon by CiPSC-islets in culture medium was measured using human C-peptide ELISA kit (ALPCO, 80-CPTHU-E10) and human glucagon ELISA kit (Mercodia, 10-1271-01) according to manufacturer instructions. ELISA was performed with three technical replicates for culture samples.

Human infectious pathogens in CiPSC-islets were checked by real-time quantitative PCR. The pathogens tested were Epstein-Barr virus (EBV), hepatitis A virus (HAV), hepatitis B virus (HBV), hepatitis C virus (HCV), human immunodeficiency virus type 1 (HIV1), human papilloma virus (HPV) etc. In addition, infectious pathogens potentially originating from mouse or bovine sourced cell culture materials were also tested, including bovine adenovirus (BAV), bovine parainfluenza virus (BPIV), bovine papillomavirus (BPV), bovine viral diarrhea virus (BVDV), bovine reovirus (DRV), bovine rabies virus (RV), feet shedding virus (FSV), hemorrhagic fever virus (HFV), lymphocyte choroid plexus meningitis virus (LCV), mouse adenovirus (MAV), mouse leukemia virus (MLV), mouse pneumonia virus (MPV), type III reovirus (RTIII). The *in vitro* infectious pathogen co-culture test and *in vivo* infectious pathogen test were conducted at a third-party facility, Wuhan Canvest Biotechnology (report number: 012300281-1, 012300281-2) using the same methods as that used in QC testing of the patient's CiPSC-#8.

We performed droplet digital PCR (dd-PCR) to verify biosafety of patient CiPSCs-islets. dd-PCR was evaluated for copy number of lncRNA LNCPRESS2 and LINC00678 to investigate potential contamination of the CiPSC-islets with residual PSCs cells, which have tumorigenic potential. lncRNAs LNCPRESS2 and LINC00678 have been demonstrated to show specificity to stem cell marker gene expression.[34] Dd-PCR methods can resolve a single residual undifferentiated CiPSC in 10^6 CiPSCs-islets. In addition, mycoplasma contamination, sterility and endotoxin levels were checked according to protocols in the Chinese pharmacopoeia (2020 version).

In vivo tumorigenicity tests prior to clinical transplantation of patient CiPSC-islets were performed on 50 immunodeficient SCID/Beige mice. 2×10^6 cells of CiPSC-islets were injected into mice, and tumor formation was evaluated at 4 months post-transplant. If the mice survived with no tumors, they were sacrificed to measure the sizes of the transplants and major organs at 4 months. Matrigel without 2BS cells and with ascitic fluid or CiPSC-#8 was injected as negative and positive controls, respectively. The samples were stored by fixation and embedded in paraffin for pathologic analysis.

The transportation procedure from the manufacturing site to the clinical use site took about 24 hours, and the temperature throughout transport was monitored and recorded at 2 min intervals. The average temperature was -196.2°C, with highest temperature at -190.7°C and lowest temperature at -196.4°C respectively. The transportation stability of the product was validated for quality according to the requirements in Table S1 Part 3 after the transportation processes.

Whole genome/exome sequencing (WGS/WES)

Genomic DNA was isolated from the patient's ADSCs, CiPSCs and fully differentiated CiPSC-islets. In brief, whole genome/exome sequencing libraries were prepared from genomic DNA using the HiPure Universal DNA Kit (Magen). Whole genome libraries were generated using Hieff NGS® Ultima Pro DNA Library Prep Kit for Illumina (Yeasen), whole exome libraries were generated using SureSelect XT HS2 DNA reagent kit (Agilent). Clean fastq reads were aligned to reference human genome build GRCh38 using BWA-MEM 0.7.10[66] with default parameters. Base quality score recalibration (BQSR) and PCR deduplication were performed using GATK 4.2.5.0. Single nucleotide variations (SNV), insertion and deletion variations (INDEL) were called using the haplotypecaller module of GATK. Low-confidence variants were filtered as follows: DP <10 or AD <3 for WGS and DP <50 or AD <5 for WES.

Then, variants of SNV/INDELs were annotated using ANNOVAR software.[67] Analysis of pathogenicity and carcinogenicity of SNV/INDELs was conducted based on ClinVar databases (https://www.ncbi.nlm.nih.gov/clinvar/, 20221231) and COSMIC databases (https://cancersangerac.uk/cosmic., v97). Cancer-associated mutations were first surveyed using Catalogue of Somatic Mutations in Cancer (COSMIC) v97. When the variants had been registered in COSMIC, we then evaluated whether the variant functioned as a cancer driver mutation using the Cancer Gene Census list available in COSMIC, listed in Table S1 Part 5. In addition, disease-related human variations were annotated using ClinVar, a public archive of reports of human variations classified for diseases and drug responses.

Single cell RNA-sequencing analysis

To further analyze the characteristics of patient CiPSC-islets and compare them to primary human islets, we performed single cell RNA-sequecing analysis of cells sampled from cell preparation prior to transplant.

Using Chromium Next GEM Single Cell 3' Kit v3.1 (10x Genomics, 1000268) and Chromium Next GEM Chip G Single Cell Kit (10x Genomics, 1000120), the cell suspension (700–1200 living cells per μL determined by Count Star) was loaded onto the Chromium single cell controller (10x Genomics) to generate single-cell gel beads in the emulsion according to the manufacturer's protocol.

In brief, CiPSC-derived islets were dissociated into single cells using Accutase, collected and resuspended at 1 × 10^6 cells per mL in 1× PBS with 0.04% BSA. About 8 × 10^3 cells were added to each channel, and the target cell to be recovered was estimated to be about 5 × 10^3 cells. Captured cells were lysed and the released RNA was barcoded through reverse transcription in individual gel beads in emulsion (GEMs). Reverse transcription was performed on a T100 Touch Thermal Cycler (Bio-Rad) at 53 °C for 45 min, followed by 85 °C for 5 min, and then held at 4 °C. The cDNA was generated and then amplified, and quality-assessed using the Qsep1 system. According to the manufacturer's instructions, scRNA-sequencing libraries were constructed using the Library Construction Kit. The libraries were quality-assessed using the Qsep1 system. The libraries were finally sequenced using the Illumina NovaSeq 6000 sequencer with a sequencing depth of at least 2 × 10^5 reads per cell with a paired-end 150 bp (PE150) reading strategy.

Single-cell RNA pre-processing

The clean reads of patient CiPSC-islets were aligned to human reference genome GRCh38 using Cell Ranger 7.2.0. The output filtered matrices were loaded into R and performed pre-process using R package.[68] In detail, doublet detection was performed using scDblFinder. Cells that met any of the criteria below were regarded as low-quality cells and removed from analysis: (1) number of expressed gene less than 200, (2) total UMI counts less than 500, (3) percentage of mitochondrial UMI counts more than 20%, (4) $\log_{10}$(doublet score + 1) more than 0.6. After that, normalization, PCA dimensional reduction, clustering, and UMAP dimensional reduction were performed using Seurat[65] following standard pipeline. Cell clusters with low quality and no unique marker were removed as part of a second round of quality control. The remaining high quality cell clusters were annotated based on known islet markers.

Integration with human pancreatic data

We downloaded human pancreatic data from GSE114297 and performed pre-processing in the same method described above. We performed integration following pipeline of RPCA integration using Seurat. Then, the integrated expression matrix was used to perform UMAP dimensional reduction.

Short-tandem repeat (STR) analysis

STR analyses were contracted out at Beijing Microread Genetics. In brief, the genomic DNA was used for PCR using the STR Multi-amplification Kit (Microreader 21 ID System) and analyzed using the ABI 3730xl DNA Analyzer (Applied Biosystems) and GeneMapperID-X software.

Immunofluorescence

Immunofluorescence analysis was performed as previously described.[4] After fixation with 4% paraformaldehyde (DingGuo) at room temperature for 30 min, cells were permeabilized and blocked with PBST solution, PBS containing 0.1% Triton X-100 (Sigma-Aldrich) and 2% donkey serum (Jackson Immuno Research) at 37 °C for 1 h. Primary antibody incubation at the appropriate dilutions was performed at 4 °C overnight in the same buffer. The next day, cells were washed three times with PBS and incubated with secondary antibodies in PBS containing 2% donkey serum at 4 °C overnight. Cells were then washed three times with PBS and DNA was stained with DAPI solution (Roche Life Science).

For frozen aggregate sections, cell aggregates were washed with PBS and fixed with 4% PFA for 2 h at 4 °C, then washed three times with PBS and dehydrated overnight at 4 °C in 30% sucrose solution. The samples were overlaid with OCT (Sakura, 4583) solution and frozen using liquid nitrogen and stored at −80 °C. A freezing microtome was used to cut 10-μm sections, which were placed on slides. The slides were washed with PBS and permeabilized with PBST solution for 1 h at room temperature. The slides were then stained with primary and secondary antibodies as immunofluorescence analysis. Antibody details are provided in key resources table.

Teratoma formation

For teratoma formation, patient CiPSC-#8 colonies were dispersed by ReLeSR and collected before injection. Approximately 2 × 10^6 cells were resuspended in Matrigel and then subcutaneously injected to male immunodeficient NPG mice (aged 2 to 3 months) that were purchased from the Beijing Vitalstar Biotechnology Company. Teratomas were observed by 8 weeks, which were then embedded in paraffin. The paraffin sections were stained with haematoxylin and eosin. All of the mouse experiments performed were approved by the Institutional Animal Care and Use Committee of Peking University.

RT–qPCR analysis

Total RNA was isolated using the Direct-zol RNA MiniPrep Kit (Zymo Research, R2053). cDNA was synthesized from 0.5 μg of total RNA using TransScript First-Strand cDNA Synthesis SuperMix (TransGen Biotech, AT311-03). qPCR was performed using the KAPA SYBR FAST qPCR Kit Master Mix (KAPA Biosystems, KM4101) on the CFX Connect Real-Time System (Bio-Rad). The data were analysed using the ΔΔCt method. GAPDH was used to normalize the expression of target genes. A list of the primer sequences for qPCR in this study is provided in key resources table.

Transplantation in mouse model

Six-to-eight-week-old SCID/Beige mice were purchased from Beijing Vital River Laboratory Animal Technology Company. The mice were housed on a 12-h light/dark cycle in a temperature-controlled room (22 ± 1 °C) with 40–60% humidity.

Transplantation into STZ-treated diabetic mice

Diabetes was induced as previously reported by five consecutive days of 16-h fast followed by intraperitoneal (i.p.) injection of 70 mg/kg of STZ (Selleck, S1312) daily. Approximately 3 × 10^6 CiPSC-islets cells were transplanted under the left kidney capsule. Fasting blood glucose levels after 16-h fasting were monitored weekly by tail bleed using a handheld glucometer (Roche, 06870279001). Body weights of animals were measured weekly. Glucose-stimulated human C-peptide secretion was assessed by collecting blood samples after 16-h fast and at 30 min after glucose injection (2 g/kg, 30% solution, i.p.). For glucose tolerance tests, i.p. injection of glucose (2 g/kg, 30% solution) was performed after 16-h fasting, and blood glucose levels were monitored at the predetermined time points (0 min, 5 min, 15 min, 30 min, 60 min, 90 min and 120 min). Plasma was frozen at −80 °C until human C-peptide analysis.

Transplantation into non-STZ-treated healthy mice

Approximately 3 × 10^6 CiPSC-islet cells were transplanted under the left kidney capsule. Blood sample after a 16-h fast was collected for fasting human C-peptide measurement. Plasma was frozen at −80 °C until human C-peptide analysis. ELISA was performed with two technical replicates owing to limited blood samples from mouse.

Flow cytometry

CiPSC-islets were released into a single-cell suspension with Accutase (Thermo, 00-4555-56) and then stained for NK6 homeobox 1 (NKX6.1), C-peptide, Glucagon (GCG), Somatostatin (SST), chromogranin A (CHGA), and tryptophan hydroxylase 1 (TPH1) as described previously.[21] Single cells were fixed with Fixation/Permeabilization Solution (BD BioSciences, 554714) for 20 min at 4°C, then washed twice in BD Perm/Wash™ Buffer (1×) and incubated with primary antibodies overnight at 4 °C. Primary antibodies were diluted with wash buffer (1×). Cells were washed twice in BD Perm/Wash™ Buffer (1×) and incubated with secondary antibodies for 1 h at 4 °C. Cells were then washed twice in BD Perm/Wash™ Buffer (1×) and analyzed using BD Accri C6 Plus. FlowJo version 10 software was used for flow cytometry analysis. Antibody details are provided in the key resources table.

Glucose stimulated insulin secretion (GSIS) assay

Preparation of Krebs buffer was as follows: 129 mM NaCl, 4.8 mM KCl, 2.5 mM $CaCl_2$, 1.2 mM $MgSO_4$, 1 mM Na_2HPO_4, 1.2 mM KH_2PO_4, 5 mM $NaHCO_3$, 10 mM HEPES, and 0.1% bovine serum albumin were dissolved in deionized water, and sterile-filtered before use. 100 CiPSC-islets were pretreated in 1 mL of 2.8 mM low-glucose Krebs solution for 1 h at 37°C, followed by sequential treatment with 1 mL low-glucose Krebs solution (2.8 mM) for 1 h, high-glucose Krebs solution (16.7 mM) for 1 h and KCl (30 mM) for 30 min. Immediately after incubation, aliquots of supernatant were collected separately, and measured using an insulin ELISA kit (Mercodia, Uppsala, Sweden). 100 CiPSC-islets were lysed by sonication with 100 μL RIPA buffer (Thermo Fisher Scientific, 89900, Waltham, MA, USA) on ice. Total protein concentration were measured using a BCA protein assay kit (Solarbio, Beijing, China). Insulin contents in low/high-glucose/KCl were presented after being normalized by the total protein. Insulin secretion of islets was expressed as the glucose-stimulated index (GSI; insulin secretion at high glucose/insulin secretion at low glucose).

Cell preparation and subanterior rectus sheath transplantation

CiPSC-islet cell recovery and preparation was conducted at the clinical site under GMP-level conditions. On day 0, 40 cryopreserved vials of CiPSC-islet cells (1.8 × 10^8 cells per vial) were thawed in a 37 °C water bath. Cell suspension was then transferred into a 50 mL centrifuge tube containing 30 mL of DMEM-basic medium (Gibco, 11054020), followed by centrifugation at 400 g for 5 min. Cells were resuspended in CMRL1066 (Corning, 15-110-CV) supplemented with 0.25% human serum albumin (HAS, CSL Behring, 113615) and 10 μM Y27632 (Selleckchem, S1049). Viability and yield were verified by trypan blue (Invitrogen, T10282) and Countess II Automated Cell Counter (Invitrogen, AMQAX1000). Then, the cells were seeded at 6 × 10^6 cells per well (not per microwell) in six-well AggreWell™400 Microwell Plates (STEMCELL Technologies, 27940) for aggregation. A total of 100 AggreWell plates were used for aggregation. After incubating in 5% CO at 37 °C for 20 h, on day 1, the clusters were collected and suspended in CMRL1066 medium. Suspended aggregates were cultured in low-adhesion six-well plates in a shaking incubator at a rotation rate of 90 r.p.m. at 37 °C, 5% CO2 and 85% humidity before transplantation on day 3.

During this time before transplantation, the items in *Quality control and final check of CiPSC-islets preparation before transplantation* (as shown in Table S1 Part 3) were tested as a final check. CiPSC-islet morphology and purity were confirmed using dithizone (DTZ) stain and microscopic evaluation, and the viability of CiPSC-islets was tested by fluorescein diacetate (FDA) / propidium iodide (PI) staining. Flow cytometry was performed in dissociated cells for islet endocrine cell-related markers (NKX6.1, C-peptide, GCG, SST). Glucose stimulated insulin secretion (GSIS) assay was conducted to evaluate the Glucose Stimulation Index (GSI) of functional potency. Thorough testing of the final CiPSC-islets was conducted to detect for residues of concern, including residual BSA and cytokines.

A total of 1,488,283 IEQ (19,843 IEQ/Kg) CiPSC-islets were transplanted into this patient on June 25th, 2023 (based on prior experience, 1 IEQ contains approximately 1348.5 ± 187.6 CiPSC-islet cells). The tissue volume of CiPSC-islets was 6 mL, resuspended in saline supplemented with 5% human serum albumin and loaded into syringes with a suspension volume of 2 mL each. The patient underwent general anesthesia, and then the abdominal skin was sterilized. Under guidance of ultrasound, a puncture

was performed from the outer edge of the rectus abdominis muscle using an 18-gauge puncture needle with an inner diameter of 1 mm (Leapmed, Suzhou, China). The direction of the needle was from the lateral side towards the abdominal midline. Once the needle tip reached between the anterior rectus sheath and rectus abdominis muscle, it was horizontally positioned and maintained in that orientation while proceeding with further medial insertion. After reaching the target position, the CiPSC-islets were injected as the puncture needle was simultaneously slowly withdrawn. As a result, the CiPSC-islets were dispersed in and around the needle tract. The length of the trajectory in which the islets were infused was 3–4 cm. A total of 7 injections were performed in parallel. A new needle was used after the 4th injection, and a total of 2 needles was used for the entire procedure. Any remaining cells in the needle were destroyed.

Immunosuppression and other medications

Before CiPSC-islets transplantation, the patient was maintained on immunosuppressive therapy with tacrolimus (2-2.5 mg/day), mycophenolate mofetil (1 g/day) and methylprednisolone tablets (8 mg/day) due to liver transplantation. For CiPSC-islets transplantation, Basiliximab (20 mg) was used for induction therapy on day 0 and day 4. Etanercept was administrated intravenously on day 0 (50 mg) and subcutaneously on day 3, day 7 and day 10 (25 mg) to alleviate inflammatory reactions. For maintenance therapy, the previously described immunosuppressive maintenance regimen for liver transplantation was continued. Cefazolin Sodium was administered for infection prophylaxis during the perioperative period.

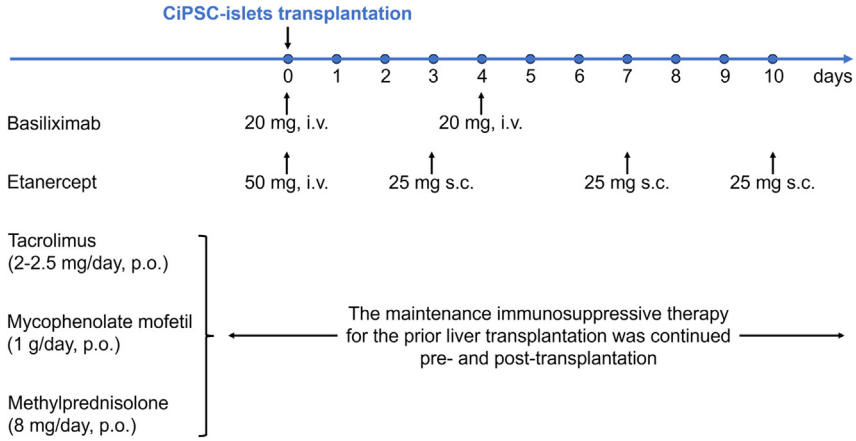

i.v.: Intravenous drop infusion
s.c.: Subcutaneous injection
p.o.: Oral administration

Laboratory methods

Patient's peripheral venous blood was collected for HbA1c and C-peptide testing at each study visits. HbA1c was analyzed by high-performance liquid chromatography (Bio-Rad). The patient's continuous blood glucose level was monitored with FreeStyle Libre system (Abbott). The glucose tolerance test was performed by orally administering a 75 g glucose solution in the fasted state (minimum 8h fast). Peripheral venous blood samples were collected at fasted state and at 0.5, 1, 2, and 3 h post-administration for the measurement of glucose and C-peptide concentrations. Blood glucose and C-peptide levels were measured by chemistry analyzer (Roche, Cobas C701) and electrochemiluminescence (Roche, Cobas e8000), respectively. The tacrolimus concentration in the blood sample was measured using the Architect Tacrolimus assay (Abbott, Architect i1000SR immunoassay analyzer) (Figure S4C). The β-HCG levels in blood specimens were determined using an automated immunology analyzer (Roche, cobas e602). The concentration of circulating tumor markers were measured by electrochemiluminescence (Roche, Cobas e8000). Detection of diabetes autoantibodies in blood involves the use of chemiluminescence for GADA, IAA, and ICA, radioligand binding method for IA-2Ab, and immunoblotting for ZnT8.

QUANTIFICATION AND STATISTICAL ANALYSIS

BETA-2 score calculation

The BETA-2 score, which used fasting metabolic variables, was derived and validated by Peter Senior, Shareen Forbes, and colleagues from individuals transplanted in the Edmonton Islet Transplantation Program and is widely used in the clinical assessment of graft function after islet transplantation. In this study, BETA-2 scores were calculated based on the formula *beta* − *2 score* $= \frac{\sqrt{\text{fasting C}-\text{peptide }(nmol/L)\times(1-\text{insulin dose }(units/kg)}}{\text{fasting blood glucose }(mmol/L)\times\text{HbA1c }(\%)} * 1000$.[69]

ADDITIONAL RESOURCES

TJFCH-iPS-001: An exploratory clinical study of islet-like cell transplantation differentiated from autologous induced pluripotent stem cells for the treatment of type 1 diabetes. https://www.chictr.org.cn/aboutEN.html Chinese Clinical Trial Registry: ChiCTR2300072200.

Supplemental figures

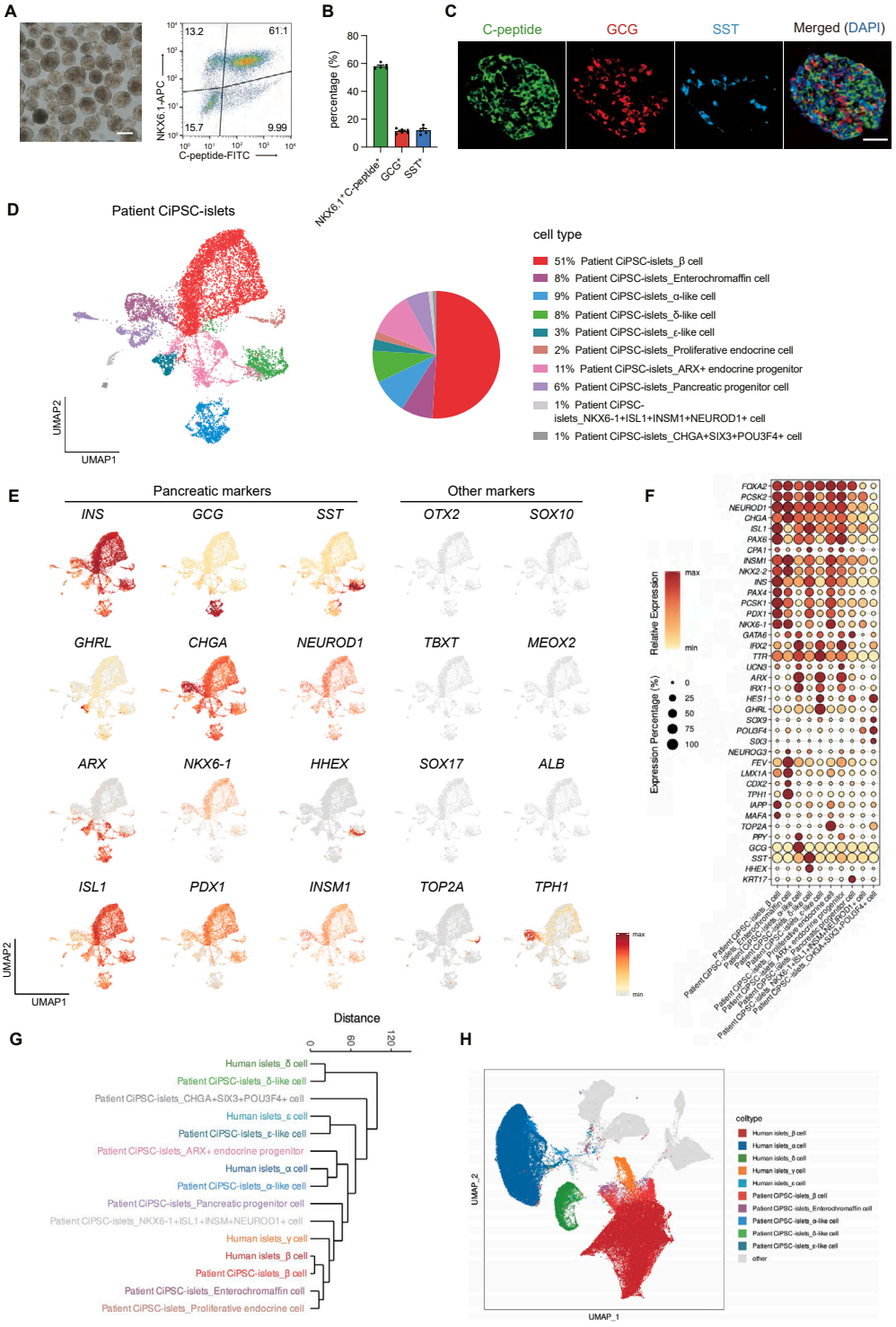

(legend on next page)

Figure S1. Characterization of patient CiPSC-islets, related to Figure 1

(A) Left: representative bright-field image of patient CiPSC-islet aggregates at stage 6. Scale bar, 200 μm. Right: representative flow cytometry analysis of the expression of β cell markers in stage 6 aggregates.

(B) Proportions of islet hormone-positive cells in stage 6 aggregates, detected by flow cytometry (n = 6). Data presented as mean ± S.E.M.

(C) Representative immunofluorescence staining of islet hormones in sectioned stage 6 aggregates. Scale bar, 50 μm.

(D) Left: UMAP projections of recovered CiPSC-islets (before transplantation) showing cell populations identified through single-cell RNA sequencing. Right: proportions of subpopulations present in patient CiPSC-islets, as identified from single-cell RNA sequencing. The existence of the four major pancreatic endocrine cell populations and their proportions, which were 51% β cells, 9% α-like cells, 8% δ-like cells, and 3% ε-like cells, were confirmed, and the remaining cells comprised pancreatic progenitors (∼6%), proliferative endocrine cells (∼2%), ARX+ endocrine progenitors (∼11%), and enterochromaffin cells (8%), a type of enteroendocrine cell that has been widely reported to be also generated in β cell differentiation cultures. Two minor subpopulations (∼1% each) expressing certain markers related to pancreatic lineage were identified.

(E) Expression of islet hormone genes and other endocrine transcription factors and functional genes, with an absence of mesodermal (*TBXT*/*MEOX2*) or ectodermal (*OTX2*/*SOX10*) populations and absence of endoderm progenitor (*SOX17*) and liver (*ALB*) fate populations.

(F) Dot plot showing the expression pattern of pancreatic lineage-related genes in cell subpopulations present in patient CiPSC-islets.

(G) Hierarchical clustering of global gene expression profiles of cell types present in patient CiPSC-islets generated *in vitro* (patient CiPSC-islets) and cell types present in primary human islets (human islets).

(H) Superimposed UMAP projections of patient CiPSC islets and human islets. Datasets are colored according to their assigned cell identity. Data are presented as mean values ± SEM. UMAP, uniform manifold approximation and projection.

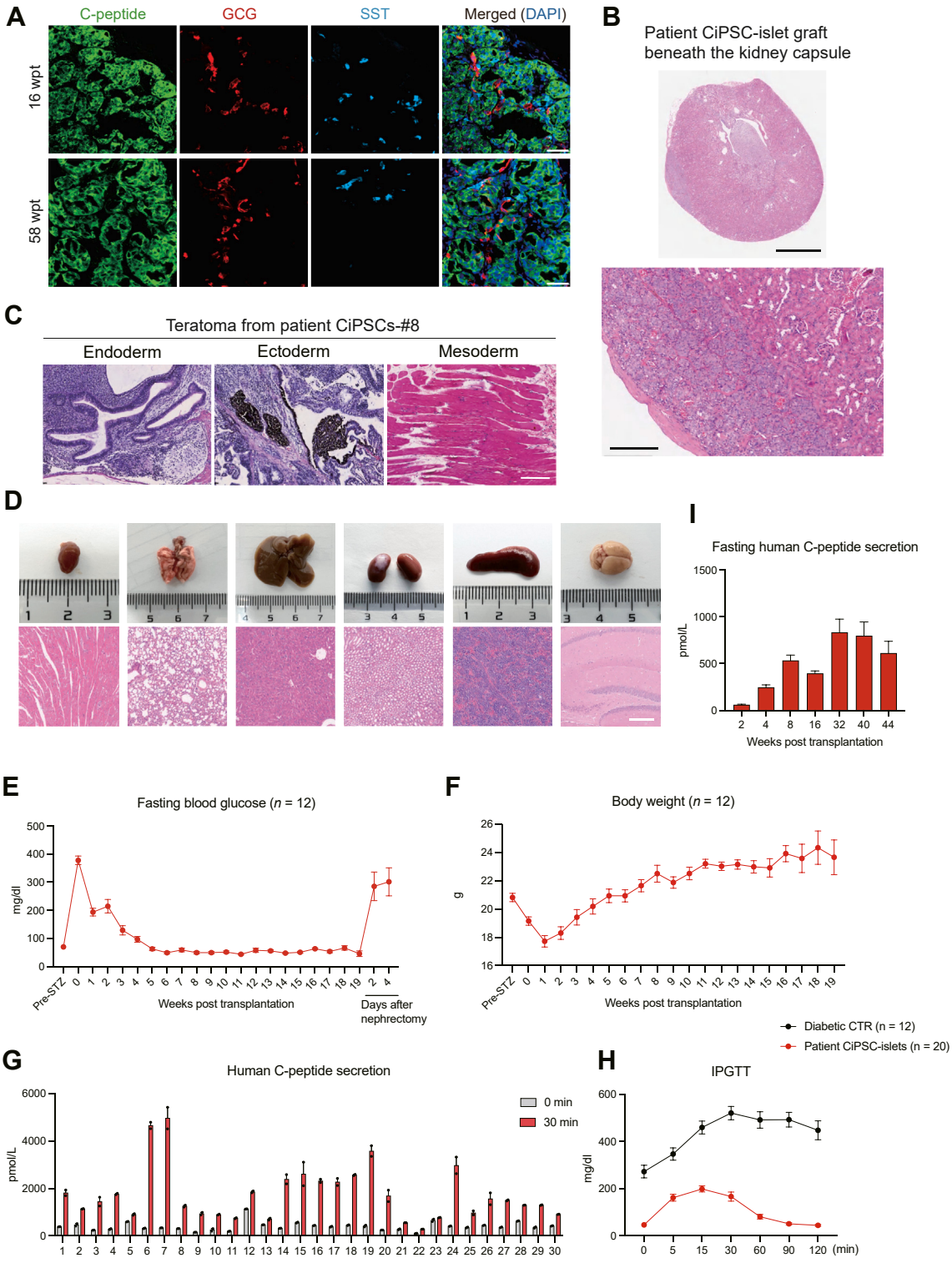

Figure S2. The patient-derived CiPSC-islets showed *in vivo* safety and efficacy in diabetic mice model, which included mice observed for an extended period of up to 58 weeks, related to Figure 1

(A) Immunofluorescence staining of islet hormones in patient CiPSC-islet graft at 16 and 58 weeks post-transplantation (wpt). Scale bar, 50 μm.

(B) Representative image of nephrectomized kidney showing the patient CiPSC-islet graft beneath the kidney capsule at 4 months after transplantation demonstrated the absence of teratoma formation. Scale bar: 1.25 mm (up) and 200 μm (down).

(legend continued on next page)

(C) Representative images of hematoxylin and eosin staining of teratoma tissue sections generated from patient CiPSC-#8 as positive control for tumorigenesis test, retrieved at 8 weeks post-transplantation into immunodeficient mice, showing endoderm (intestinal epithelium), mesoderm (muscle), and ectoderm (pigmented retinal epithelium) lineages from a single teratoma. Scale bars, 200 μm.

(D) Postmortem examination of major organs in transplanted mouse, with absence of graft-related malignancy. Gross anatomy (top) and H&E staining (bottom) of major organs at 4 months after transplantation. Scale bar, 50 μm. From left to right: heart, lung, liver, kidney, spleen, and brain. Left kidney capsule bears the CiPSC-islets graft.

(E) Fasting blood glucose levels of patient CiPSC-islet transplanted diabetic mice (n = 12). Data presented as mean ± S.E.M.

(F) Tracking of body weight of patient CiPSC-islet transplanted diabetic mice (n = 12). Data presented as mean ± S.E.M.

(G) Human C-peptide secretion in response to glucose challenge in patient CiPSC-islet transplanted mice at 16 wpt (n = 30 animals measured at two technical replicates each). Data presented as mean ± S.E.M.

(H) Changes in blood glucose levels in response to intraperitoneal glucose tolerance test (IPGTT) of STZ-induced diabetic mice groups with (n = 20) and without (n = 12) patient CiPSC-islet transplantation at 16 wpt. Data presented as mean ± S.E.M.

(I) Detection of fasting human C-peptide secretion in patient CiPSC-islet transplanted non-diabetic mice. First detection was conducted at 2 wpt (n = 10). Data presented as mean ± S.E.M.

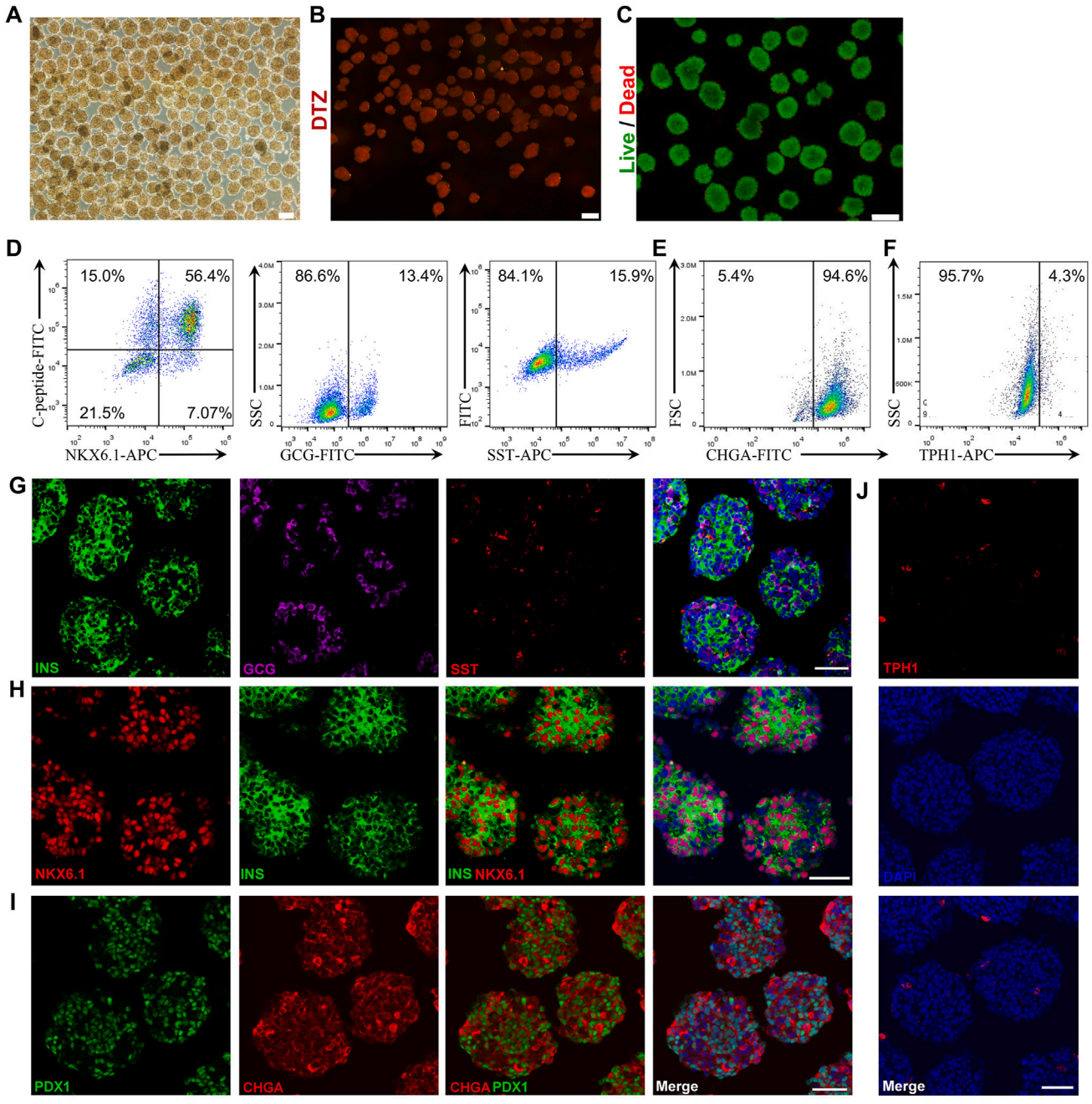

Figure S3. Pre-transplantation *in vitro* characterization of the recovered patient CiPSC-islet, related to Figure 1

(A) Representative bright-field image of CiPSC-islets. Scale bar, 200 μm.

(B) Representative bright-field image of dithizone (DTZ)-stained CiPSC-islets. Scale bar, 200 μm.

(C) Representative immunofluorescence image of live/dead analysis of CiPSC-islets using FDA/PI staining. Scale bar, 250 μm.

(D–F) Representative flow cytometry analysis of the expression of β, α, and δ cell markers (D), endocrine cell marker chromogranin A (CHGA) (E), and entero-chromaffin cell marker tryptophan hydroxylase 1 (TPH1) (F).

(G) Immunofluorescence staining of insulin, glucagon, and somatostatin, showing pancreatic endocrine cell composition of CiPSC-islets. Scale bar, 50 μm.

(H) Co-staining of NKX6.1 and insulin to confirm the NKX6.1 expression in beta cells ($INS^+NKX6.1^+$). Scale bar, 50 μm.

(I) Co-staining of PDX1 and CHGA staining to identify pancreas progenitor cells ($PDX1^+CHGA^-$) and endocrine cells ($CHGA^+$). Scale bar, 50 μm.

(J) TPH1 staining to identify SC-enterochromaffin cells ($TPH1^+$). Scale bar, 50 μm.

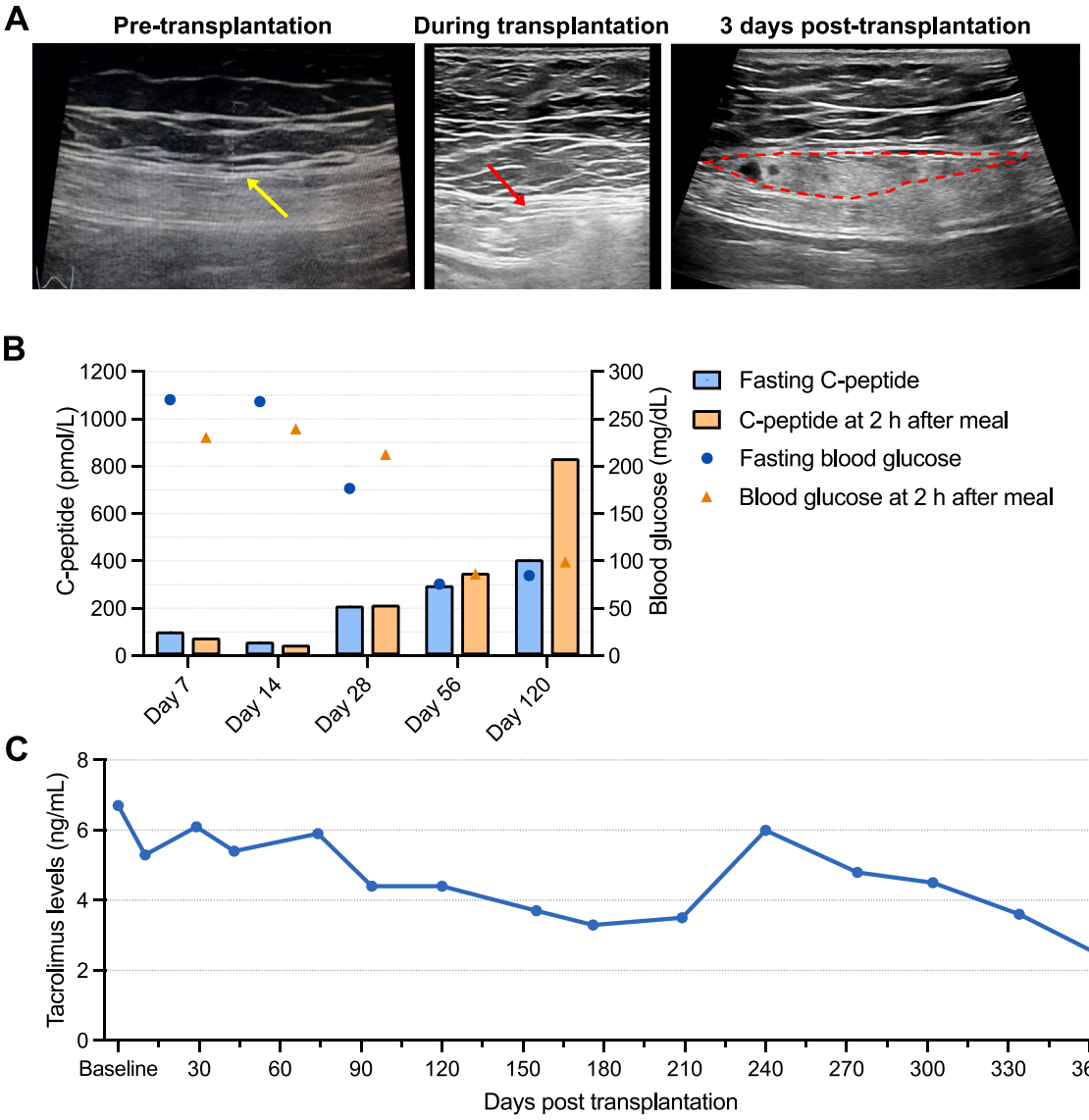

Figure S4. Transplantation process under the guidance of ultrasound, fasting, and postprandial C-peptide values and circulating tacrolimus concentrations post-transplantation, related to Figures 3 and 4

(A) Ultrasound-guided injection of CiPSC-islets into the space beneath the abdominal anterior rectus sheath. The yellow arrow indicates the rectus sheath, the red arrow points to the needle tip of the puncture needle, and the dashed line indicates the distribution area of the transplanted CiPSC-islets.

(B) Fasting and 2-h postprandial C-peptide levels and glucose levels.

(C) The circulating tacrolimus concentrations of the patient.